ARTICLE

Color Fine Tuning of Optical Materials Through Rational Design

Brigitte Holzer[a]*, Johannes Bintinger[a,b]*‡, Daniel Lumpi[a], Christopher Choi[b], Youngwan. Kim[b], Berthold Stöger[c], Christian Hametner[a], Martina Marchetti-Deschmann[c], Felix Plasser[d], Ernst Horkel[a]‡, Ioannis Kymissis[b] and Johannes Fröhlich[a]

Abstract: We report on the feasibility for color fine-tuning of optical materials using rational design principles based on chemical reasoning. For this purpose, a modular framework for the construction of symmetrical cap-linker-cap compounds, using triarylamine caps and oligothiophene linkers, is applied. The chosen structural scaffolds are heavily used in recent industrial applications and provide five possibilities for altering their electronic and steric properties: electron donor/acceptor groups, planarization/deplanarization, and modulation of the π-conjugation length. Permutation of the used building blocks leads to a set of 54 different molecules, out of which 32 are synthesized and characterized in solution as well as in example fabricated OLED devices. This setup allows for color fine-tuning in the range of 412 nm to 540 nm with typical steps of 4 nm. In addition, to further benefit from the large experimental data set the spectroscopic results are used to benchmark quantum chemical computations, which show excellent agreement thus highlighting the potential of these calculations to guide future syntheses.

Introduction

Organic light emitting diodes (OLEDs) are considered to be the next generation of both display technology and lighting applications,[1] as they offer the possibility to manufacture flexible, light weight and energy efficient devices.[2,3] Moreover, OLEDs are based on organic semiconducting materials, which can be rationally designed leading to tailor made devices regarding electrical and photophysical properties.[4–6] Hence, OLEDs have attracted much interest from both academia and industry.[7] Thiophenes have been extensively used in organic electronics (OE) as they exhibit high charge carrier mobilities.[8–12] Unfortunately, however thiophenes themselves are not suited for use in OLEDs, as they are prone to fluorescence self-quenching as a result of strong π-π stacking.[13] For this reason a common approach is to combine these thiophenes with modified triphenylamine (TPA) scaffolds, which are frequently used in OE due to their beneficial electron donor and hole transport properties.[14–18] The materials under investigation combine these structural scaffolds consisting of thiophene based linker systems and triarylamine containing cap units (Figure 1), thus leading to a material class featuring good charge carrier mobilities originating from the oligothiophene unit and improved fluorescent properties by preventing self-quenching caused by the introduction of the TPA motifs.[19,20] Each individual building block can readily be synthesized or structurally modified to meet electronic and spectroscopic requirements. In this comprehensive study we report on 5 possibilities of color tuning by molecular design of novel OLED materials (electron donating/withdrawing groups, planarization and de-planarization, extension of the π-system), which allows for a large number of possible combinations. However, the synthesis of novel organic materials is an expensive and time intense task, in which the desired outcome is often unknown until the materials are implemented and tested in real devices and applications. Thus, it would be a great advantage to have reliable knowledge regarding relevant physical properties of the materials in hand to select the most promising candidate before conducting the actual synthesis.

For the prediction of photoluminescent properties, time-dependent density functional theory (TD-DFT)[21–23] offers itself as an attractive option by providing a good compromise between computational efficiency and accuracy. The main challenge in this case is the choice of an appropriate density functional, which can dramatically affect the outcome of the calculation.[24–26] Here, we chose the M06-2X exchange-correlation functional,[27] following a number of detailed benchmark studies,[26,28–30] as well as our own experience on the substance class studied here.[31] Rather than simply computing the vertical excitations, it is of special interest to predict the entire emission spectrum for the color tuning of novel OLED compounds. This is achieved, here, by not only considering the vertical excitation energies obtained by the TD-DFT calculations but also including information regarding vibrational broadening. While in our previous work[31] smaller model compounds were investigated, we now present computations of significantly larger molecules which represent a material class which is actually used in OLEDs.[32] We show that the applied protocol provides a powerful standalone tool, which does not require any parameter fitting based on pre-known experimental

[a] Dr. B. Holzer*, Dr. J. Bintinger*,‡, Dr. D. Lumpi, Dr. C. Hametner, Dr. E. Horkel‡, Prof. J. Fröhlich
Institute of Applied Synthetic Chemistry
Vienna University of Technology
Getriedemarkt 9, 1060 Vienna
* Both authors contributed equally
E-mail: johannes.bintinger@tuwien.ac.at
ernst.horkel@tuwien.ac.at

[b] C. Choi, Y. Kim, Prof. I. Kymissis
Department of Electrical Engineering
Columbia University
500 W. 120th St., Mudd 1310, New York, 10027, USA

[c] Dr. B. Stöger, Prof. M. Marchetti-Deschmann
Institute of Chemical Technologies and Analytics
Vienna University of Technology
Getreidemarkt 9, 1060 Vienna, Austria

[d] Dr. F. Plasser
Institute for Theoretical Chemistry, Faculty of Chemistry
University of Vienna
Währinger Straße 17, 1090 Vienna, Austria

Supporting information for this article is given via a link at the end of the document

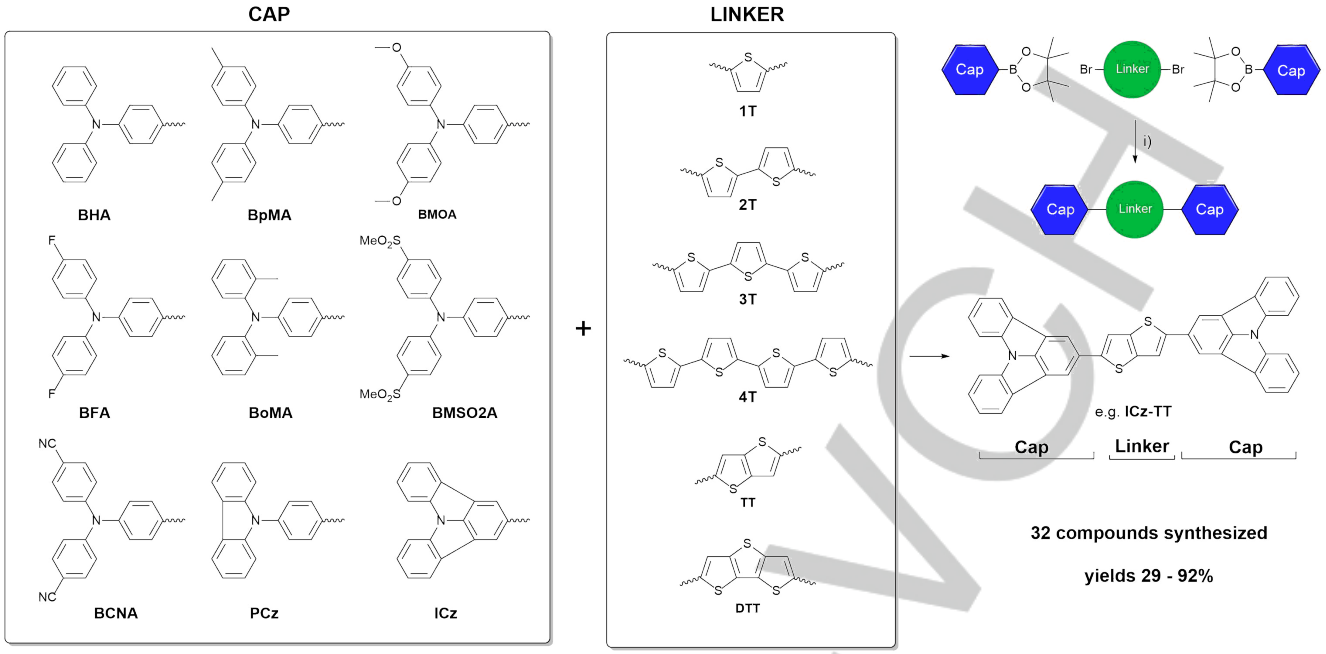

Figure 1. Molecular design of cap-linker-cap systems. Reaction conditions i): KOtBu, (IPr)Pd(allyl)Cl, IPA / water, reflux.

data to yield accurate predictions even for real world applications. To underline reliability and accuracy of the presented method, results of the computations were in turn compared with the corresponding experimentally obtained spectroscopic properties. As the correlation between simulation and experiment was very high, we feel confident to have a powerful tool in hand to rationally guide future synthesis by means of quantum chemical calculations.

Results and Discussion

Molecular design

A modular approach is highly advantageous for tailor-made compounds that are designed according to customer requirements and allows both economical synthesis and exhaustive tuning capabilities of various properties. The building blocks incorporated in the substances under investigation are thiophenes used as linkers and TPA units serving as caps. Alteration of the molecular design of triphenylamine-based materials by introducing either electron-donating or -withdrawing substituents allows fine tuning of photophysical properties of a variety of fluorescent materials.[20] Also the application of planarized or deplanarized moieties strongly influences absorption and emission characteristics.[33,34] This study aims to give conclusive insight into structure/property relationships of substance classes comprised of triphenylamines and oligothiophenes both from an experimental as well as from a computational point of view. To evaluate the electronic and steric effects of substituted triphenylamine-based materials the following strategies are applied altering the design of a cap-linker-cap system (Figure 1): introduction of both (i) electron-donating and (ii) -withdrawing substituents on the triphenylamine (TPA) cap, (iii) planarization and (iv) deplanarization of the TPA moiety by introduction of either indolocarbazole (ICz), phenylcarbazole (PCz) or ortho-methyl substituted TPA scaffolds, as well as (v) modulation of the π-linker by applying bithiophene, terthiophene, quarterthiophene as well as thieno[3,2-*b*]thiophene (TT) or dithieno[3,2-*b*:2',3'-*d*]thiophene (DTT). Permutation of caps and linkers presented in Figure 1 leads to a matrix of 54 possible compounds, out of which a representative set of 32 substances were rationally selected, synthesized and thoroughly investigated regarding their relevant properties for their use in OE applications. Furthermore, the obtained experimental data are used as valuable references for benchmarking the computational method, ultimately leading towards a powerful tool for predicting structure property relationships.

Synthesis

The synthetic linkage of triphenylamines (TPA), indolocarbazole (ICz) as well as phenylcarbazole (PCz) scaffolds and thiophene-based linkers toward symmetrical bis(triarylamines) was realized by Suzuki cross-coupling reaction. A general procedure developed in an earlier study tolerating a broad spectrum of functionalized TPA boronic acid esters[20] was applied for the synthesis of **BoMA-1T**, **BHA-2T**, **BpMA-2T**, **BMOA-2T**, **BFA-2T**, **BoMA-2T**, **PCz-2T**, **ICz-2T**, **BHA-3T**, **BpMA-3T**, **BMOA-3T**, **BFA-3T**, **BHA-4T**, **BpMA-4T**, **BMOA-4T**, **BFA-4T**, **BHA-TT**, **BoMA-TT**, **PCz-TT**, **ICz-TT**, **BHA-DTT**, **BoMA-DTT**, **PCz-DTT**, **ICz-DTT**, **PCz-1T** and **ICz-1T**. A convenient synthetic pathway for planarized TPA moieties PCz and ICz was previously described.[34] (Figure 1). The syntheses of 2,5-disubstituted thiophenes bearing various triphenylamines (**BHA-1T**, **BpMA-1T**, **BMOA-1T**, **BFA-1T**, **BSO2MA-1T** and **BCNA-1T**) have been previously described by our group.[34,35] Linker precursors including 2,5-dibrominated thiophene-, bi-, ter- and quaterthiophenes 1T-4T were synthesized according to literature,[36–38] while fused thiophene derivatives TT and DTT were obtained by a procedure as described by Frey.[39] The synthesis of the required TPA boronic ester derivatives of BHA,

BpMA, MOA, BFA, BMSO2A and BCNA for Suzuki cross-coupling was also described previously by our group.[20] All efforts to produce sterically hindered derivative BoMA via the same classical methods (eg. Ullman-condensation, Buchwald-Hartwig amination) as applied before failed. For instance, typical Ullman conditions using 4-bromoaniline and 2-iodotoluene with either CuCl/phenanthroline or $CuSO_4 \cdot 5H_2O/K_2CO_3$ yielded only trace amounts of the desired *N*-(4-bromophenyl)-bis(2-methylphenyl)benzeneamine. Hence an alternative synthetic protocol starting from 2-bromotoluene and 2-methylaniline was developed. Since Ullman and Buchwald-Hartwig based attempts failed again we started investigating a route including a nucleophilic aromatic substitution step toward **2b** (Table 1).

Table1. Synthetic pathway toward **2a-b** i): KOtBu, (IPr)Pd(allyl)Cl, toluene, reflux; ii): nucleophilic aromatic substitution.

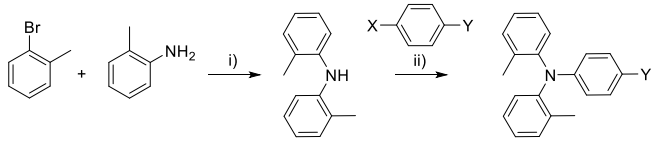

1 **2a** Y = Br **2b** Y = NO_2

Entry	X	Y	reagent	product
1	F	Br	Cs_2CO_3/K_2CO_3	-
2	F	Br	NaH	-
3	F	NO_2	Cs_2CO_3/K_2CO_3	-
4	F	NO_2	NaH	74%(isol.)

Substrate/base combinations directly aiming for the target compound **2a** (entries 1, 2) were investigated. Since these attempts were not successful, more activated substrates were chosen as starting materials applying bases with different strength (entries 3, 4). Compound **2b** could be obtained in a multigram approach in 74% yield by nucleophilic aromatic substitution applying 4-fluoronitrobenzene and sodium hydride as base. However, it is noteworthy to mention that the use of DMF as solvent is mandatory, as parallel experiments with DMSO showed inferior results. Having the nitro compound **2b** in hand the desired boronic ester derivative of BoMA was obtained by following a straight-forward route using $SnCl_2$ reduction[40], diazotization and conversion of the obtained amine **2c** to the iodo species **2d** followed by Miyaura borylation.[41] The obtained final compounds were all solid materials appearing yellow to red in color. Solubility strongly depends on linker length and planarization of the cap. In general, the higher the linker length and the greater the planarization of the compound the worse the solubility is.

The characterization of **BoMA-1T**, **BHA-2T**, **BpMA-2T**, **BMOA-2T**, **BFA-2T**, **BoMA-2T**, **PCz-2T**, **ICz-2T**, **BHA-3T**, **BpMA-3T**, **BMOA-3T**, **BFA-3T**, **BHA-4T**, **BpMA-4T**, **BMOA-4T**, **BFA-4T**, **BHATT**, **BoMA-TT**, **PCz-TT**, **ICz-TT**, **BHA-DTT**, **BoMA-DTT**, **PCz-DTT** and **ICz-DTT** was performed by ^1H / ^{13}C-NMR spectroscopy and MALDI-TOF MS analysis. All data are consistent with the proposed structural formulations.

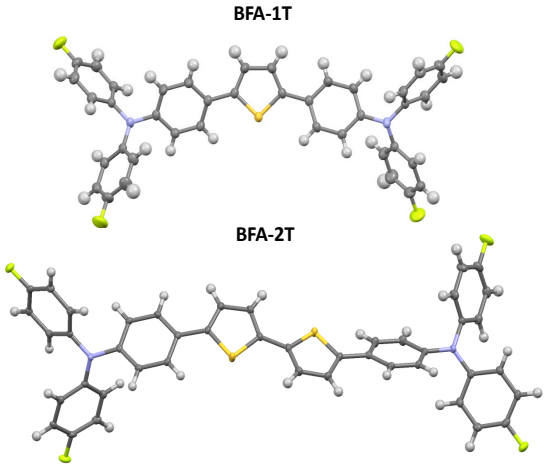

Figure 2. Molecular structures of **BFA-1T** (top) and **BFA-2T** (bottom). C, N, F and S atoms are represented by gray, blue, green and yellow ellipsoids drawn at the 50% probability levels. H atoms are represented by white spheres of arbitrary radius.

Molecular structures

Single crystals of compounds **BFA-1T** and **BFA-2T** were obtained by slow evaporation of solvent from saturated cyclohexane solutions. The crystal structures of **BFA-1T** and the cyclohexane solvate of BFA-2T were determined by single crystal diffraction (Figure. 2).

The angles between the phenyl rings of the triphenylamine moieties linked to the aromatic thiophene cores and the thiophene linker of these compounds are summarized in Table S2. In this table also a comparison of angles with those of compounds **BHA-1T**, **BHA-2T** and **BpMA-2T** is given, for which structural characterizations have already been published.[31] The benzene/thiophene angles feature a large variance, ranging from a virtually coplanar benzene/thiophene pair in **BHA-2T** [26.13(7)°]. They may be very different in the same molecule [BHA-1T: 1.21(8)° vs. 19.60(8)°] or identical in molecules located on twofold rotation axes or centers of inversion [**BFA-1T, BHA-2T**]. The geometric parameters of **BHA-2T** were determined in two solvatomorphs (MeOH and CD_2Cl_2) with a total of four crystallographically independent molecules. The large variance of the benzene/thiophene angle in even this case demonstrates that packing effects are dominant. The thiophene/thiophene twist angles in the bithiophene compounds feature an even more pronounced variance, ranging from perfectly coplanar in the **BHA-2T** molecules, which are symmetric by inversion, to 33.05(8)° in **BpMA-2T**.

Photophysical properties

As a first step of photophysical characterization fluorescence spectra in solution were recorded. These data are in particular interesting for potential OLED application, as it has been demonstrated (e.g. for BpMA-nT)[42] that photoluminescence spectra from solutions give a good first approximation for the electroluminescence spectra emitted by an OLED fabricated with

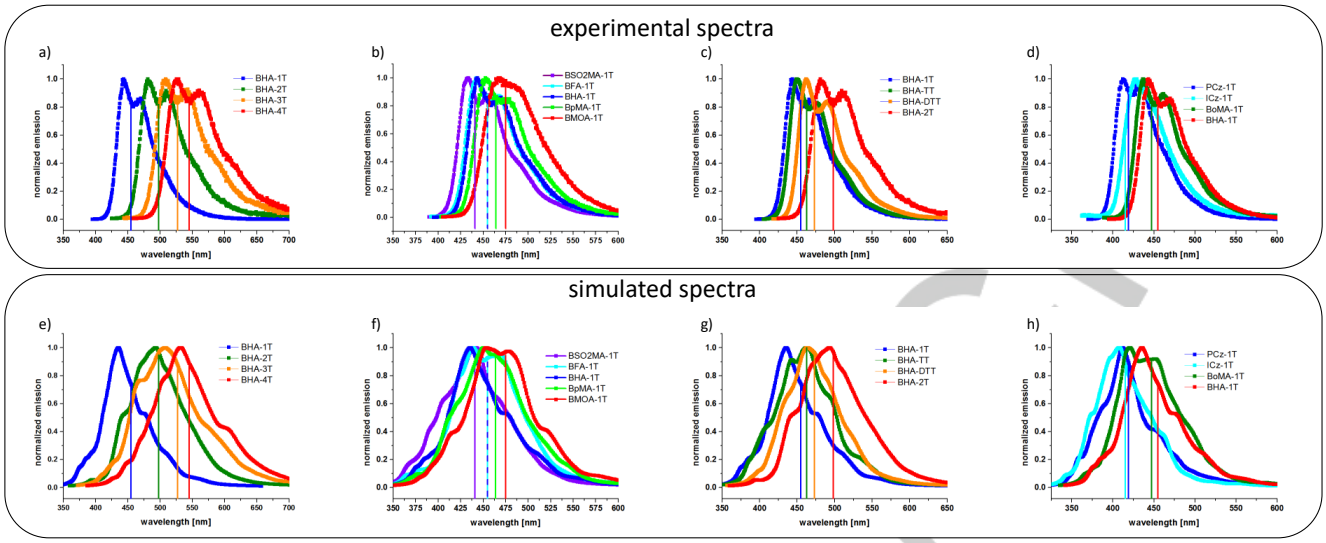

Figure 3. Overlay of fluorescence emission spectra of selected compounds from experimentally recorded from 1 µM THF solutions (a-d) and computational simulations (e-h). Vertical lines indicate the results of the SS-PCM calculations (see Table S1 $\lambda_{SS\text{-}PCM}$).

this respective compound. In the following some exemplary subsets of data are analyzed while the full set of absorption and emission spectra as well as all numerical data is given in the supporting information (Figure S49-53, Table S1).

Figure 3a illustrates an overlay of the emission spectra for compounds BHA-(1-4)T and thus demonstrates the influence of the repetitive thiophene units. As expected, two trends within oligomeric series are confirmed by the experimental data; i) there is a correlation between the bathochromic shift and the conjugation length of the linker system; ii) the extent of the bathochromic shift decreases with the number of thiophene units. (Vertical lines in Figure 3 are referring to computational results and are discussed in the respective section.) Next, the variation of the electronic properties of the cap was investigated, while keeping the linker constant (Figure 3b). Defining **BHA-1T** as a reference (lowest energy maximum of solution fluorescence; λ_1=444 nm) the influence of ±M and ±I substituents was analyzed. Consistently, electron withdrawing groups (SO_2Me, F) exhibit a hypsochromic shift whereas electron donating (Me, OMe) groups induce a bathochromic shift. Since inductive effects are in the majority of cases weaker than mesomeric ones, this fact is also being reflected in the magnitude of the spectral shift in regard to the reference. Surprisingly, the fluorine substituent (having an -I effect) exhibits only a negligible impact on the emission maximum (λ_1=442 nm) compared to the +I substituent (Me, λ_1=453 nm). Moreover, to explore other means of color tuning, planarization and deplanarization of the linkers (Figure 3c) as well the caps (Figure 3d) was investigated. In comparison to Figure 3a the effect of increasing the number of π-electron pairs within the linker unit from three (thiophene) to five (thienothiophene) only slightly increases the bathochromic shift (+6 nm). In contrast, the next analogue of the fused linker series, dithienothiophene which counts seven π-electron pairs, has an emission maximum shifted by +19 nm and +13 nm compared to **BHA-1T** and **BHA-TT** respectively. Interestingly, the compound comprising the bithiophene linker which is bearing six π-electron pairs, is far more red shifted compared to **BHA-1T** than the one containing the dithienothiophene linker (+37 nm vs. +6 nm). This is remarkable since one would expect the reverse order as dithienothiophene exhibits an elongated π-electron system. The results of planarized (ICz and PCz) and deplanarized (oMe) caps on the spectral properties of the same linker system are shown in Figure 3d in comparison to the reference compound **BHA-1T**. A clear tendency amongst all investigated compounds bearing planarized PCz and fully planarized ICz for a hyposochromic shift compared to compounds with caps exhibiting a higher degree of freedom (BHA and BoMA) can be observed. The partially planarized cap systems PCz shows a larger blue shift than the corresponding fully planarized ICz bearing compound. The most red shifted spectra are observed for the BHA caps followed by the sterically demanding cap systems BoMA. The building block-like influence of individual cap and linker systems is shown in Table 2.

Table 2. Empirical increments for the shift of the fluorescence maximum λ_1 (from Table S1) for various linkers and caps in respect to cap-reference BHA and linker reference T.

Caps			Linkers	
BpMA	+ 6 ± 2 nm		2T	+ 34 ± 3 nm
BMOA	+ 18 ± 5 nm		3T	+ 59 ± 5 nm
BFA	- 4 ± 1 nm		4T	+ 77 ± 5 nm
BoMA	- 5 ± 1 nm		TT	+ 5 ± 3 nm
PCz	- 30 ± 1 nm		DTT	+16 ± 6 nm
ICz	- 22 ± 4 nm			

This table is intended as a guideline for predicting certain trends, e.g. for the calculation of the emission of **BMOA-4T** Table 2 reads +18 nm as a contribution from BMOA and additional +77 nm from the linker elongation to four thiophene units. When both increments are added to the reference emission of **BHA-1T** (λ_1=444 nm), the result of 539 nm is in very good agreement with the experimentally obtained value of 540 nm. As only selected cap-linker combinations were synthesized and tested, one must be careful when applying these empirical increments to

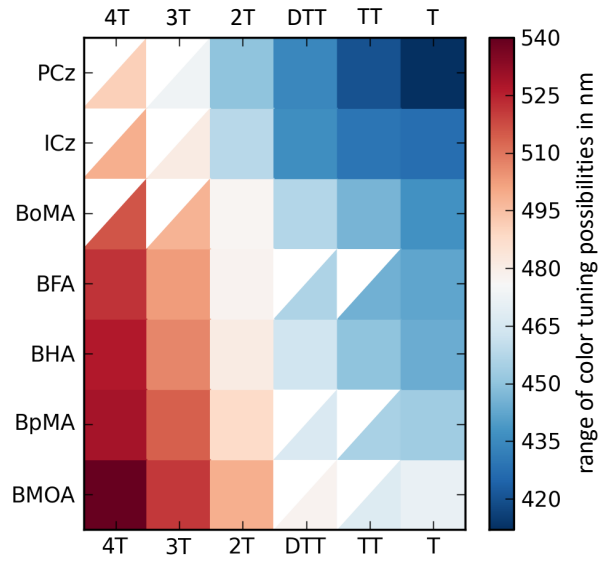

Figure 4. Pseudo color plot of emission maximum λ_1 in nm of substances under investigation. Full squares represent experimental values while half colored squares express incremented values.

combinations outside the scope of this library. However, data of Table 2 suggests that variation of cap and linker contribute independently to the observed emission shift based on the reference **BHA-1T**. A graphical representation of Table 2 is depicted in Figure 4. The graph illustrates the broad range of colors accessible by the employed color tuning methods. From Figure 4 it is even more evident that it is advantageous to apply relative small linkers (T, TT and DTT) and planarized caps (PCz, ICz) to obtain bluish colors. On the other hand extended π-linker system (3T, 4T) combined with caps bearing electron donating groups (BMOA, BpMA) are suitable for more reddish colors.

Theoretical calculations

In our previous study we evaluated a reliable procedure for the prediction of emission spectra of bis(aminophenyl)-substituted thiophene derivatives.[31] While the initial development was mainly based on simple model compounds, we also applied the complete procedure to one larger molecule in order to test the scope of the method. Inspired by the promising results, we are now expanding the predictive tools to a much broader set of real OLED compounds. To get a first insight on the molecular structures, ground state and first excited state geometries were optimized by means of density functional theory (DFT) and time-dependent (TD) DFT calculations using a parametrization which was optimized during the initial studies.[31] In Figure 5 the optimized geometries of both ground state (S0) and the first excited state (S1) of selected compounds **BHA-3T**, **PCz-1T**, **ICz-1T** and **ICz-DTT** are presented. Two observations stand out when analyzing the molecular structures. An increasing curvature of the oligothiophene linkers in the 1-4T series is seen for S0 geometries while in contrast the molecules' central core (thiophene units and the two adjacent phenyl rings) is being completely planarized in S1. This holds true also for the other compounds, resulting in the case of ICz-derivatives in a completely planarized structure in S1. For comprehensive illustration of additional compounds and their S0 and S1 geometries see supporting information (Figure S62-66). Molecular orbital distributions of S0 for selected compounds **BHA-1T**, **BMOA-1T**, **BMSO2A-1T**, **PCz-1T** and **ICz-1T** are shown in Figure 6. For all compounds, the HOMO is distributed over the entire molecule. The effect of the electron donating/withdrawing groups is clearly visible, resulting in a higher/lower electron density in the outer phenyl rings of the caps

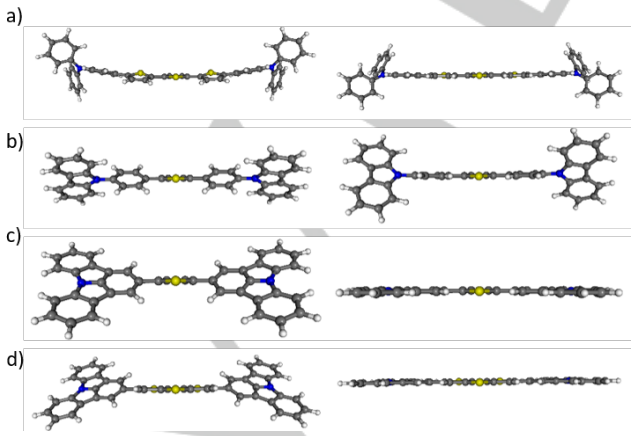

Figure 5. Optimized geometries of **BHA-3T** (a), **PCz-1T** (b), **ICz-1T** (c) and **ICz-DTT** (d) (M06-2X/SVP, LR-PCM/THF); left: S0, right S1.

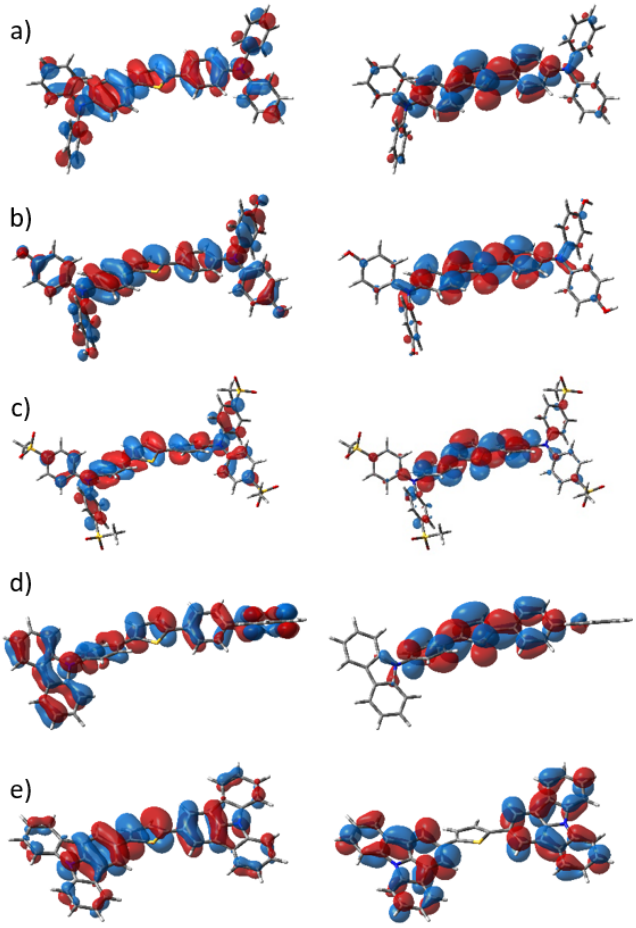

Figure 6. Molecular orbital plots for selected compounds **BHA-1T** (a), **BMOA-1T** (b), **BMSO2A-1T** (c), **PCz-1T** (d) and **ICz-1T** (e) (M06-2X/SVP, LR-PCM/THF); left: HOMO, right LUMO

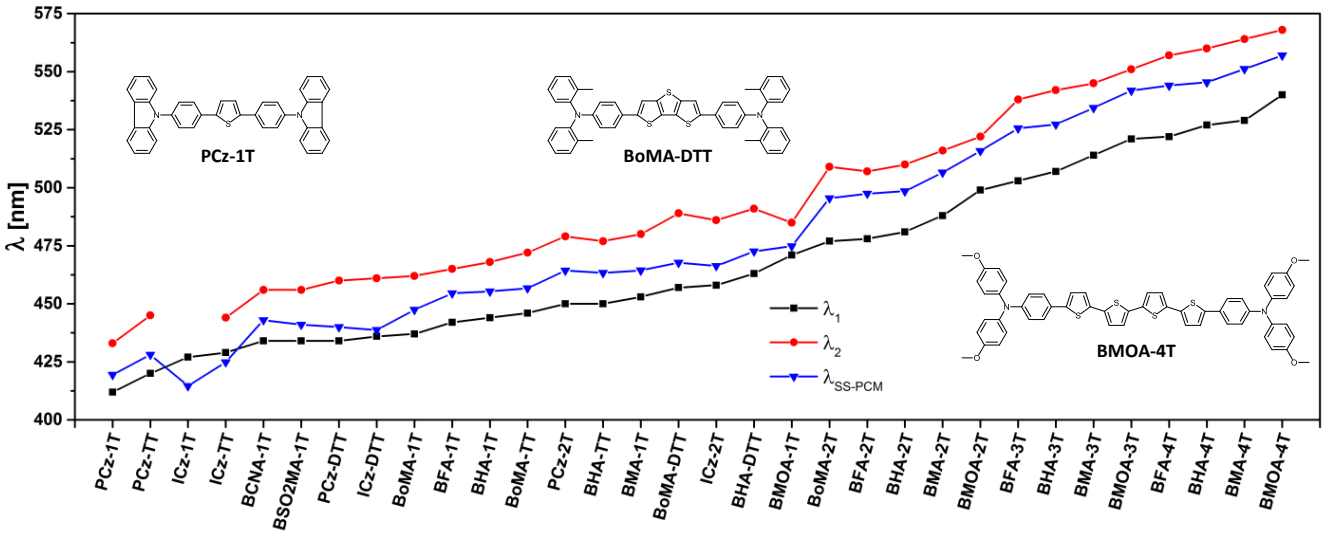

Figure 7. Comparison for all compounds of λ_1 = highest energy maximum of solution fluorescence; λ_2 = lowest energy maximum of solution fluorescence; $\lambda_{SS\text{-}PCM}$ = calculated vertical emission.

in **BMOA-1T**/**BMSO2A-1T**, respectively. In the case of the partially planarized PCz cap, an almost uniform distribution of the electron density is obtained. In contrast, **ICz-1T** does not exhibit this uniformity, as the electron density is decreased on the phenyl rings not directly connected to the thiophene linker. Generally, the LUMOs are predominantly localized on the central core of the molecules (thiophene linker plus the adjacent phenyl rings). However, in the case of fully planarized ICz bearing compounds the LUMO is exclusively localized on the ICz moiety.

This finding is in agreement with our previous studies on ICz containing compounds, where it was shown that ICz is not necessarily an electron donor, but also exhibits electron accepting properties.[34,43,44]

For additional HOMO/LUMO plots, the interested reader is referred to the supporting information (Figure S67-82). To make computational results comparable with experimental data it is imperative to consider solvent effects, hence they were included through the polarizable continuum model (PCM)[45] in its linear response (LR-PCM)[46] and state specific (SS-PCM)[47] formulations. For a detailed discussion of the performance of these two solvent models we refer the reader to the works of Corni *et al.*[48] and Caricato *et al.*[49] while a discussion of alternative solvation models was presented by Daday *et al.*[50] and Budzák *et al.*[51] For the present work, the SS-PCM is chosen, following our previous study,[31] which showed superior performance of SS-PCM over LR-PCM for the class of systems studied here. As already observed,[31] the computed vertical emissions using SS-PCM are always in between the two maxima of the recorded spectra in THF solutions (Table S1) which is graphically illustrated in Figure 7. To obtain simulated spectra in solution we used a somewhat more sophisticated protocol (see Section 5.3 for details) to obtain spectra including both the accurate SS-PCM correction and vibrational broadening (Figure 3e-h and Figure S57-61). As a result, a robust procedure for the fluorescence spectra simulation of medium to large size oligothiophene derivatives is now available and is in turn benchmarked against experimental data, ultimately leading towards a powerful tool for predicting structure property relationships. Figure 3 illustrates the comparison between computational results (e-h, both vertical emissions and simulated spectra) and experimentally obtained fluorescence spectra (a-d, for the complete set of data, the reader is referred to Table S1, while all comparison graphs can be found in the supporting information Figure S57-61). Generally spoken all results indicate a good agreement between experimental and computational data. As mentioned above the calculated vertical emissions (SS-PCM) are always located in between the two emission maxima, except for some ICz bearing compounds (Figure 7). Figure 7 also illustrates that using the employed caps and linkers it is possible to fine tune the emission wavelength down to several nm. As shown in Figure 8 the spectral simulations match consistently with the experimental spectra, however while the red onset of the spectral simulation fits very well with the measurements, the blue part is somehow overestimated in the simulation. In order to obtain more application-relevant data, emission spectra from OLEDs, fabricated using a selected subset of compounds, were recorded and compared to both experimental and simulated spectra. Some graphs are shown in Figure 8, for additional graphs the reader is referred to the supporting information (Figure S54-S55). Figure 9 demonstrates

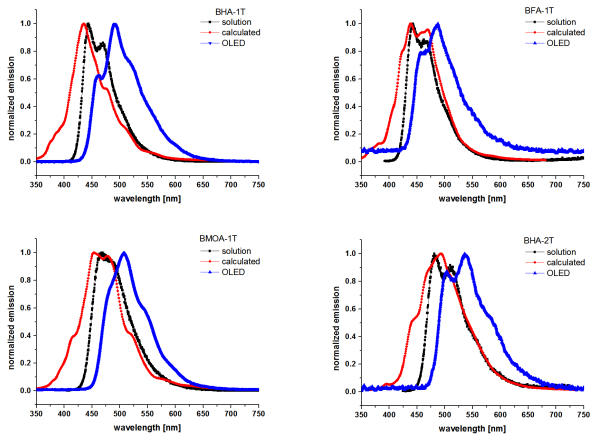

Figure 8. Selected examples for the comparison of experimental (solution and OLED) and simulated fluorescence spectra. Solution refers to fluorescence measured from 1 µM THF solution.

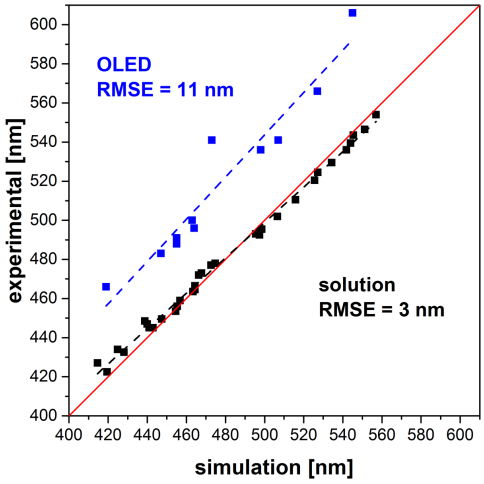

Figure 9. Correlation between experimental data (λ_{av} and λ_{OLED}) and computational results ($\lambda_{SS\text{-}PCM}$) compared to the ideal correlation (45° line, red). First order regression are plotted as dashed lines.

the correlation between experimental data and computational results for the entire data set. Each data point represents one compound; calculated values are plotted on the x-axis, while the experimental data are plotted on the y-axis. The resulting graph shows nearly ideal correlation (represented by the red 45° line) of computational and experimental data from solution covering all compounds and their emission characteristics under investigation. A root mean square error (RMSE) of only 3 nm is estimated for the calculation ($\lambda_{SS\text{-}PCM}$) in respect to the regression of the solution based emissions (λ_{av}). A first order regression applied to the OLED data set yields a straight nearly parallel to the 45 ° line. As a result, OLED spectra exhibit a relatively constant red shift of about +42 nm in respect to the calculated emissions, whereas the RMSE of the OLED emissions in respect to the regression is 11 nm. This is of great value for material design since the simulation can now be also used for the estimation of the OLED spectra as only a constant shift has to be added to the computed value.

These results strengthen our confidence in the power of this methodology to accurately predict emission spectral properties covering a large variety of different compounds, composed of miscellaneous structural motifs only by means of computational chemistry.

Conclusions

Five possibilities of color tuning for cap-linker-cap type OLED materials were investigated by means of a combined experimental and theoretical approach. The individual building blocks used for synthesis offer the possibility to alter both electronic (electron donating/withdrawing groups, extension of the π-system) and steric (planarization and deplanarization) properties of the resulting compounds. A comprehensive set of 32 molecules was synthesized and the final materials were characterized regarding their photophysical properties in addition to the implementation of selected compounds into OLED devices. The investigated compounds showed emissions between 412 nm and 540 nm in fairly even intervals, demonstrating the possibility of color fine-tuning based on chemical reasoning. The cap and linker groups showed additive effects on the emission that could be assigned according to a clear increment system. In parallel to experimental work, a recently presented computational method was further optimized in order to predict and simulate the entire emission spectra of organic compounds, meaning that not only the vertical emission is calculated, but additionally the vibrational broadening is considered.

In summary, we have demonstrated that chemical reasoning in combination with computational chemistry can be a powerful tool for rationally guiding synthesis and thus reducing synthetic efforts in the field of materials research.

Experimental Section

Materials and methods

Substances purchased from commercial sources were used as received without further purification. 2-Methylaniline, 2-bromotoluene, 4-fluoronitrobenzene and pinacolborane were purchased from Apollo Scientific. Allyl[1,3-bis(2,6-diisopropylphenyl)imidazol-2-ylidene]chloropalladium(II) ((IPr)Pd(allyl)Cl, CAS 478980-03-9),[52] [1,1'-bis(diphenylphosphino)ferrocene]dichloro-palladium(II) ($PdCl_2$(dppf), CAS 72287-26-4),[53] 2,5-dibromothiophene (CAS 3141-27-3),[37] 5,5'-dibromo-2,2'-bithiophene (CAS 4805-22-5),[36] 2,5-dibromothieno[3,2-*b*]thiophene,[54] 5,5'-dibromo-2,2':5',2''-terthiophene,[38] 2,6-dibromodithieno[3,2-*b*:2',3'-*d*]thiophene (CAS 67061-69-2)[55] and 5,5'''-dibromo-2,2':5',2'':5'',2'''-quaterthiophene, *N,N*-Bis(4-fluorophenyl)-4-(4,4,5,5-tetramethyl-1,3,2-dioxaborolan-2-yl)benzene-amine,[20] 2-(4,4,5,5-tetramethyl-1,3,2-dioxaborolan-2-yl)indolo[3,2,1-*jk*]carbazole[34] and 9-[4-(4,4,5,5-tetramethyl-1,3,2-dioxaborolan-2-yl)phenyl]-9*H*-carbazole[56,57] were synthesized according to literature. 4,4'-(2,5-Thiophenediyl)bis[*N,N*-diphenylbenzenamine], 4,4'-(2,5-thiophenediyl)bis[*N,N*-bis(4-methylphenyl)benzenamine], 4,4'-(2,5-thiophenediyl)bis[*N,N*-bis(4-fluorophenyl)benzenamine], 4,4',4',4'''-[2,5-thiophenediylbis(4,1-phenylene)dinitrilo] tetrakis[benzonitrile] and 4,4'-(2,5-thiophenediyl)bis[*N,N*-bis[4-(methylsulfonyl)-phenyl] benzenamine] were synthesized as described elsewhere.[35] Anhydrous *N,N*-dimethylformamide was purchased from Aldrich Chemical Co. Anhydrous dioxane was prepared immediately prior to use by a PURESOLV-plant (it-innovative technology inc.). Isopropylalcohol (IPA), acetonitrile (ACN) and dimethylsulfoxide (DMSO) were used in p.a. quality. Technical grade solvents (dichloromethane (DCM)) were distilled prior to use. Anhydrous solvents were prepared by filtration through drying columns. Analytical TLC was performed on Merck silica gel 60 F254 plates. Chromatographic separations at preparative scale were carried out on silica gel (Merck silica gel 60, 40 - 63 µm). Nuclear magnetic resonance (NMR) spectra were obtained using a Bruker DPX-200 or Avance DRX-400 fourier transform spectrometer operating at the following frequencies: DPX-200: 200.1 MHz (^{1}H) and 50.3 MHz (^{13}C); DRX-400: 400.1 MHz (^{1}H) and 100.6 MHz (^{13}C). The chemical shifts are reported in delta (δ) units, parts per million (ppm) downfield from tetramethylsilane using solvent residual signals for calibration. Coupling constants are reported in Hertz; multiplicity of signals is indicated by using following abbreviations: s=singlet, d=doublet, t=triplet, q=quartet. The multiplicity of ^{13}C signals was obtained by measuring JMOD spectra. UV-Vis absorption spectra and fluorescence emission spectra were recorded in THF solutions (1 µg/mL) with a Perkin Elmer Lambda 750 spectrometer and an Edinburgh FLS920, respectively. High-resolution mass spectra (HRMS) were acquired as radical cations using either a SYNAPT HDMS instrument (Waters, Manchester, UK) equipped with a matrix-assisted laser desorption/ionization (MALDI) source or a Thermo Scientific LTQ Orbitrap XL hybrid FTMS (Fourier Transform Mass Spectrometer) equipped with Thermo Fischer Exactive Plus Orbitrap (LC-ESI+) and a Shimadzu IT-TOF Mass Spectrometer. Samples for MALDI-HRMS were applied at 1 mg/mL in THF on stainless steel using

nitroanthracene (3 mg/mL in THF) as MALDI matrix. In case of solubility the sample was further diluted to approx. 50 pg/µL. In case of undissolved samples the slurry was centrifuged and the supernatant and the residue was used for MALDI-qTOF-MS analysis. 1 µL of the sample or residue/chloroform slurry was deposited on a stainless steel target and dried at room temperature. The samples were measured by laser desorption/ionization (LDI) on a Synapt HDMS G2 (Waters, UK) using a 200Hz YAG laser in V-mode. All MS spectra were recorded as accurate mass data with angiotensin II (m/z = 1046.542) as internal lock mass achieving a mass accuracy of 15 - 40 ppm (i.e. ∆m/z = 0.01 - 0.04 amu). X-ray Structure Determination. Crystals of **BFA-1T** (CCDC#1473931) and the cyclohexane solvate of **BFA-2T** (CCDC#1476440) were grown by slow evaporation of solutions in cyclohexane. X-ray diffraction data were collected at T = 180 K (**BFA-1T**) and T = 100 K (**BFA-2T**) in a dry stream of nitrogen Bruker Smart APEX (**BFA-1T**) and Kappa APEX II (**BFA-2T**) diffractometer systems using graphite-monochromatized Mo-Kα radiation (λ = 0.71073 Å) and fine sliced φ- and ω-scans. Data were reduced to intensity values with SAINT and an absorption correction was applied with the multi-scan approach implemented in SADABS.[58] The structures were solved by charge flipping implemented in SUPERFLIP[59] and refined against F with JANA2006.[60] Non-hydrogen atoms of the title molecules were refined anisotropically. The C atoms of the cyclohexane solvent molecule, which is disordered around a center of inversion, were refined with isotropic displacement parameters. The H atoms were placed in calculated positions and thereafter refined as riding on the parent atoms. Molecular graphics were generated with the program MERCURY.[61] Bottom emitting OLEDs were fabricated via thermal evaporation onto clean glass pre-patterned indium tin oxide (ITO) cathodes under high vacuum (10^{-6} torr). 50 nm of the novel OLED compounds were evaporated directly onto the ITO-patterned glass at a rate of 0.6 Å/s to form the emissive layer where recombination of charge carriers produces luminescent photons. A 15 nm thick layer of bathocuproine (BCP) was then deposited at a rate of 0.3 Å/s as a hole blocking layer. Following this, 35 nm of tris (8-hydroxyquinolinato) aluminum (AlQ_3) was deposited at a rate of 0.6 Å/s as the electron transport layer. Finally, the cathode consisted of 1 nm LiF, evaporated at 1 Å/s, followed by aluminum, evaporated at 0.8 Å/s. A schematic layout of the devices is given in the supporting information. The devices were powered using a Keithly 2400 source measurement unit, and the spectrum was recoreded with a USB-4000 spectrometer.

Synthetic Details

General procedure for the synthesis of **BoMA-1T**, **PCz-1T**, **ICz-1T**, **BHA-2T**, **BpMA-2T**, **BMOA-2T**, **BFA-2T**, **BoMA-2T**, **PCz-2T**, **ICz-2T**, **BHA-3T**, **BpMA-3T**, **BMOA-3T**, **BFA-3T**, **BHA-4T**, **BpMA-4T**, **BMOA-4T**, **BFA-4T**, **BHA-TT**, **BoMA-TT**, **PCz-TT**, **ICz-TT**, **BHA-DTT**, **BoMA-DTT**, **PCz-DTT** and **ICz-DTT** according to Marion.[62] Under an argon atmosphere, dibromo derivatives of 1T-4T, TT and DTT (1.0 eq.), boronic ester (3.0 eq.) and KOtBu (3.0 eq.) were suspended in a 3 : 1 mixture of IPA : H_2O (degassed by bubbling with argon). A solution of (IPr)Pd(allyl)Cl (0.02 eq.) in degassed IPA was added and the reaction mixture was refluxed, monitoring the conversion by TLC. After completion, the reaction mixture was distributed between water and chloroform; the phases were separated and the aqueous layer was extracted with chloroform three times. The combined organic layer was dried over anhydrous sodium sulfate and the solvent removed under reduced pressure to give the crude product. Purification was achieved by column chromatography.

4,4'-(2,5-Thiophenediyl)bis[*N,N*-bis(2-methylphenyl) benzenamine] - **BoMA-1T**

According to the general procedure **BoMA-1T** was synthesized applying 2,5-dibromothiophene (242 mg, 1.0 mmol, 1.0 eq), boronic ester of BoMA (1198 mg, 3.0 mmol, 3.0 eq), KOtBu (337 mg, 3.0 mmol, 3.0 eq) and (IPr)Pd(allyl)Cl (11.4 mg, 20 µmol; dissolved in 2 mL IPA). The reaction mixture was refluxed until complete conversion (1 h). After standard workup the crude product was loaded upon silica gel (3 g) and column chromatography (90 g silica gel) using light petroleum : DCM = 10 - 40% followed by crystallization from cyclohexane yielded **BoMA-1T** as bright yellow solid (571 mg, 91%). R_f = 0.26 (light petroleum : DCM = 2 : 1). ^{1}H NMR (400 MHz, CD_2Cl_2): δ = 7.42 (4 H, d, J = 8.8 Hz), 7.23 (4 H, dd, J = 6.9, 1.61 Hz), 7.08 - 7.18 (10 H, m), 6.99 (4 H, d, J = 7.3 Hz), 6.63 (4 H, d, J = 8.8 Hz), 2.05 (12 H, s) ppm. ^{13}C NMR (100 MHz, CD_2Cl_2): δ = 148.5 (s), 146.2 (s), 142.9 (s), 135.4 (s), 132.3 (d), 129.4 (d), 128.0 (d), 127.5 (d), 126.9 (s), 126.5 (d), 125.6 (d), 123.1 (d), 120.2 (d), 19.2 (q) ppm. MS (MALDI-TOF): calcd for $C_{44}H_{38}N_2S$: 626.2756; found: 626.2611.

9,9'-[(2,5-Thiophenediyl)di-4,1-phenylene]bis(9*H*-carbazole) - **PCz-1T**

According to the general procedure **PCz-1T** was synthesized applying 2,5-dibromothiophene (480 mg, 2.0 mmol, 1.0 eq), bornonic ester of PCz (2216 mg, 6.0 mmol, 3.0 eq), KOtBu (670 mg, 6.0 mmol, 3.0 eq) and (IPr)Pd(allyl)Cl (23 mg, 20 µmol; dissolved in 2 mL IPA) in a mixture of 15 mL IPA : H_2O (3 : 1). The reaction mixture was refluxed until complete conversion (2 h). After standard workup the crude product was loaded upon silica gel (8 g) and column chromatography (90 g silica gel) using light petroleum : DCM = 5 - 30% followed by crystallization from $CHCl_3$ yielded **PCz-1T** as yellow solid (475 mg, 42%). ^{1}H NMR (400 MHz, CD_2Cl_2): δ = 8.18 (4 H, d, J = 7.7 Hz), 7.93 (4 H, d, J = 8.4 Hz), 7.65 (4 H, d, J = 8.4 Hz), 7.53 - 7.42 (10 H, m), 7.35 (4 H, t) ppm. ^{13}C NMR (100 MHz, CD_2Cl_2): δ = 143.6 (s), 141.3 (s), 137.5 (s), 133.7 (s), 128.0 (d), 127.5 (d), 126.6 (d), 125.4 (d), 124.0 (s), 120.8 (d), 120.6 (d), 110.4 (d) ppm. MS (MALDI-TOF): calcd for $C_{40}H_{26}N_2S$: 566.1817; found: 566.1833.

2,2'-(2,5-Thiophenediyl)bis(indolo[3,2,1-*jk*]carbazole) - **ICz-1T**

According to the general procedure **ICz-1T** was synthesized applying 2,5-dibromothiophene (242 mg, 1.0 mmol, 1.0 eq), boronic ester of ICz (1100 mg, 3.0 mmol, 3.0 eq), KOtBu (337 mg, 3.0 mmol, 3.0 eq) and (IPr)Pd(allyl)Cl (11 mg, 20 µmol; dissolved in 2 mL IPA) in a mixture of 40 mL IPA : H_2O (3 : 1). The reaction mixture was refluxed until complete conversion (1 h). After standard workup the product was purified by crystallization from pyridine yielding **ICz-1T** as yellow solid (489 mg, 87%). ^{1}H NMR (400 MHz, CD_2Cl_2): δ = 8.44 (4 H, s), 8.23 (4 H, d, J = 7.9 Hz), 7.97 (4 H, d, J = 8.2 Hz), 7.62 (4 H, t, J = 7.6 Hz), 7.54 (2 H, s), 7.42 (4 H, t, J = 7.5 Hz) ppm. ^{13}C NMR (100 MHz, CD_2Cl_2): δ = 145.7, 139.8, 131.0, 130.4, 127.8, 124.5, 123.9, 122.6, 119.3, 118.3, 113.0 ppm. MS (MALDI-TOF): calcd for $C_{40}H_{22}N_2S$: 562.1504; found: 562.1453.

4,4'-(2,2'-Bithiophene-5,5'-diyl)bis(*N,N*-diphenylbenzenamine) - **BHA-2T**

According to the general procedure **BHA-2T** was synthesized applying 5,5'-dibromo-2,2'-bithiophene (324 mg, 1.0 mmol, 1.0 eq), boronic ester of BHA (1114 mg, 3.0 mmol, 3.0 eq), KOtBu (337 mg, 3.0 mmol, 3.0 eq) and (IPr)Pd(allyl)Cl (11 mg, 20 µmol; dissolved in 2 mL IPA) were suspended in a mixture of 15 mL degassed IPA : H_2O (3 : 1). The reaction mixture was refluxed until complete conversion (2 h). After standard workup the reaction mixture was loaded upon silica gel (7 g) and column chromatography (90 g silica gel) using light petroleum : DCM = 15 - 40% followed by crystallization from cyclohexane yielded **BHA-2T** as yellow crystals (555 mg, 85%). Rf = 0.19 (light petroleum : DCM = 5 : 1).^{1}H NMR (200 MHz, CD_2Cl_2): δ = 7.48 (4 H, d, J = 8.6 Hz), 7.22 - 7.35 (8 H, m), 7.00 - 7.18 (20 H, m) ppm. ^{13}C NMR (50 MHz, CD_2Cl_2): δ = 148.0 (s), 148.0 (s), 143.4 (s), 136.4 (s), 129.9 (d), 128.4 (s), 126.8 (d), 125.2 (d), 124.9 (d), 124.0 (d), 123.8 (d), 123.5 (d) ppm. MS (MALDI-TOF): calcd for $C_{44}H_{32}N_2S_2$: 648.1694; found: 648.1630.

4,4'-(2,2'-Bithiophene-5,5'-diyl)bis[*N,N*-bis(4-methylphenyl) benzenamine] - **BpMA-2T**

According to the general procedure **BpMA-2T** was synthesized applying 5,5'-dibromo-2,2'-bithiophene (324 mg, 1.0 mmol, 1.0 eq), boronic ester of BpMA (1198 mg, 3.0 mmol, 3.0 eq), KOtBu (337 mg,

3.0 mmol, 3.0 eq) and (IPr)Pd(allyl)Cl (11 mg, 20 µmol; dissolved in 2 mL IPA) were suspended in a mixture of 20 mL degassed IPA : H_2O (3 : 1). The reaction mixture was refluxed until complete conversion (1.5 h). After standard workup the crude product was loaded upon silica gel (6 g) and column chromatography (90 g silica gel) using cyclohexane : DCM = 8 - 16% followed by crystallization from cyclohexane yielded **BpMA-2T** as light orange crystals (619 mg, 87%). ^{1}H NMR (200 MHz, CD_2Cl_2): δ = 7.43 (4 H, J = 8.8 Hz, d), 7.16 - 7.05 (12 H, m), 7.04 - 6.92 (12 H, m), 2.32 (12 H, s) ppm. ^{13}C NMR (50 MHz, CD_2Cl_2): δ = 148.5 (s), 145.5 (s), 143.5 (s), 136.1 (s), 133.7 (s), 130.5 (d), 127.4 (s), 126.7 (d), 125.4 (d), 124.8 (d), 123.2 (d), 122.6 (d), 21.1 (q) ppm. MS (MALDI-TOF): calcd for $C_{48}H_{40}N_2S_2$: 708.2633; found: 708.2445.

4,4'-(2,2'-Bithiophene-5,5'-diyl)bis[*N,N*-bis(4-methoxyphenyl) benzenamine] - **BMOA-2T**

According to the general procedure **BMOA-2T** was synthesized applying 5,5'-dibromo-2,2'-bithiophene (324 mg, 1.0 mmol, 1.0 eq), boronic ester of BMOA (1294 mg, 3.0 mmol, 3.0 eq), KOtBu (337 mg, 3.0 mmol, 3.0 eq) and (IPr)Pd(allyl)Cl (11 mg, 20 µmol; dissolved in 2 mL IPA) were suspended in a mixture of 16 mL degassed IPA : H_2O (3 : 1). The reaction mixture was refluxed until complete conversion (1.5 h). After standard workup the crude product was loaded upon silica gel (6 g) and column chromatography (90 g silica gel) using light petroleum : diethyl ether = 5 - 100% followed by crystallization from cyclohexane yielded **BMOA-2T** as yellow solid (646 mg, 84%). ^{1}H NMR (200 MHz, CD_2Cl_2): δ = 7.39 (4 H, d, J = 8.8 Hz), 7.13 - 7.01 (12 H, m), 6.94 - 6.80 (12 H, m), 3.79 (12 H, s) ppm. ^{13}C NMR (50 MHz, CD_2Cl_2): δ = 156.8 (s), 149.0 (s), 143.6 (s), 141.1 (s), 135.9 (s), 127.4 (d), 126.6 (d), 126.3 (s), 124.7 (d), 122.8 (d), 120.7 (d), 115.3 (d), 56.0 (q) ppm. MS (MALDI-TOF): calcd for $C_{48}H_{40}N_2O_4S_2$: 772.2429; found: 772.2386.

4,4'-(2,2'-Bithiophene-5,5'-diyl)-bis(*N,N*-bis[4-fluorophenyl] benzenamine) - **BFA-2T**

According to the general procedure **BFA-2T** was synthesized applying 5,5'-dibromo-2,2'-bithiophene (324 mg, 1.0 mmol, 1.0 eq), boronic ester of BFA (1222 mg, 3.0 mmol, 3.0 eq), KOtBu (337 mg, 3.0 mmol, 3.0 eq) and (IPr)Pd(allyl)Cl (11 mg, 20 µmol; dissolved in 2 mL IPA) were suspended in a mixture of 16 mL degassed IPA : H_2O (3 : 1). The reaction mixture was refluxed until complete conversion (1.5 h).). After standard workup the crude product was loaded upon silica gel (6 g) and column chromatography (90 g silica gel) using cyclohexane : DCM = 8 - 15% followed by crystallization from cyclohexane yielded **BFA-2T** as yellow solid (613 mg, 85%). ^{1}H NMR (200 MHz, CD_2Cl_2): δ = 7.46 (4 H, d, J = 8.8 Hz), 7.18 - 6.92 (24 H, m) ppm. ^{13}C NMR (50 MHz, CD_2Cl_2): δ = 159.7 (s, J_{CF} = 242.3 Hz), 148.1 (s), 144.1 (s, J_{CF} = 2.9 Hz), 143.3 (s), 136.4 (s), 128.1 (s), 127.0 (d, J_{CF} = 7.8 Hz), 126.9 (d), 124.9 (d), 123.4 (d), 122.8 (d), 116.7 (d, J_{CF} = 22.5 Hz) ppm. MS (MALDI-TOF): calcd for $C_{44}H_{28}F_4N_2S_2$: 724.1630; found: 724.1567.

4,4'-(2,2'-Bithiophene-5,5'-diyl)-bis(*N,N*-bis[2-methylphenyl] benzenamine) - **BoMA-2T**

According to the general procedure **BoMA-2T** was synthesized applying 5,5'-dibromo-2,2'-bithiophene (324 mg, 1.0 mmol, 1.0 eq), boronic ester of BoMA (1198 mg, 3.0 mmol, 3.0 eq), KOtBu (337 mg, 3.0 mmol, 3.0 eq) and (IPr)Pd(allyl)Cl (11 mg, 20 µmol; dissolved in 2 mL IPA) were suspended in a mixture of 15 mL degassed IPA : H_2O (3 : 1). The reaction mixture was refluxed until complete conversion (2 h). After standard workup the crude product was loaded upon silica gel (6.5 g) and column chromatography (90 g silica gel) using light petroleum : DCM = 10 - 40% followed by crystallization from cyclohexane yielded **BoMA-2T** as yellow solid (495 mg, 70%). Rf = 0.38 (light petroleum : DCM = 3 : 1). ^{1}H NMR (400 MHz, CD_2Cl_2): δ = 7.41 (4 H, d, J = 8.77 Hz), 7.24 (4 H, dd, J = 7.0, 1.46 Hz), 7.07 - 7.19 (12 H, m), 7.00 (4 H, d, J = 7.0 Hz), 6.64 (4 H, d, J = 8.5 Hz), 2.06 (12 H, s) ppm. ^{13}C NMR (100 MHz, CD_2Cl_2): δ = 148.8, 146.1, 143.7, 136.0, 135.5, 132.3, 128.1, 127.6, 126.7, 126.4, 125.7, 124.7, 122.9, 120.1, 19.2 ppm. MS (MALDI-TOF): calcd for $C_{48}H_{40}N_2S_2$: 708.2633; found: 708.2604.

9,9'-([2,2'-Bithiophene]-5,5'-diyldi-4,1-phenylene)bis(9*H*-carbazole) - **PCz-2T**

According to the general procedure **PCz-2T** was synthesized applying 5,5'-dibromo-2,2'-bithiophene (648 mg, 2.0 mmol, 1.0 eq), boronic ester of PCz (2216 mg, 6.0 mmol, 3.0 eq), KOtBu (673 mg, 6.0 mmol, 3.0 eq) and (IPr)Pd(allyl)Cl (23 mg, 40 µmol; dissolved in 2 mL IPA) were suspended in a mixture of 40 mL degassed IPA : H_2O (3 : 1). The reaction mixture was refluxed until complete conversion (2 h). After standard workup the crude product was purified by crystallization from pyridine yielding **PCz-2T** as yellow goldish solid (951 mg, 73%). ^{1}H NMR (400 MHz, CD_2Cl_2): δ = 8.17 (4 H, d, J = 7.6 Hz), 7.89 (4 H, d, J = 8.5 Hz), 7.64 (4 H, d, J = 8.5 Hz), 7.39 - 7.52 (10 H, m), 7.26 - 7.35 (6 H, m) ppm. ^{13}C NMR (100 MHz, CD_2Cl_2/CS_2): δ = 142.3 (s), 140.5 (s), 137.0 (s), 136.9 (s), 132.9 (s), 127.3 (d), 126.9 (d), 126.0 (d), 124.9 (d), 124.5 (d), 123.4 (s), 120.2 (d), 120.1 (d), 109.8 (d) ppm. MS (MALDI-TOF): calcd for $C_{44}H_{28}N_2S_2$: 648.1694; found: 648.1630.

2,2'-([2,2'-Bithiophene]-5,5'-diyl)bis(indolo[3,2,1-*jk*]carbazole) - **ICz-2T**

According to the general procedure **ICz-2T** was synthesized applying 5,5'-dibromo-2,2'-bithiophene(324 mg, 1.0 mmol, 1.0 eq), boronic ester of ICz (1100 mg, 3.0 mmol, 3.0 eq), KOtBu (337 mg, 3.0 mmol, 3.0 eq) and (IPr)Pd(allyl)Cl (11 mg, 20 µmol; dissolved in 2 mL IPA) were suspended in a mixture of 30 mL degassed IPA : H_2O (3 : 1). The reaction mixture was refluxed until complete conversion (2 h). After standard workup the product was purified by crystallization from pyridine yielding **ICz-2T** as yellow solid (403 mg, 62%). MS (MALDI-TOF): calcd for C44H24N2S2: 644.1381; found: 644.1346.

4,4'-(2,2':5',2''-Terthiophene-5,5''-diyl)bis(*N,N*-diphenyl benzenamine) - **BHA-3T**

According to the general procedure **BHA-3T** was synthesized applying 5,5'-dibromo-2,2':5',2''-terthiophene (406 mg, 1.0 mmol, 1.0 eq), boronic ester of BHA (1114 mg, 3.0 mmol, 3.0 eq), KOtBu (337 mg, 3.0 mmol, 3.0 eq) and (IPr)Pd(allyl)Cl (11 mg, 20 µmol; dissolved in 2 mL IPA) were suspended in a mixture of 28 mL degassed IPA : H_2O (3 : 1). The reaction mixture was refluxed until complete conversion (1.5 h). After standard workup the crude product was loaded upon silica gel (7 g) and column chromatography (90 g silica gel) using cyclohexane : DCM = 7 - 30% followed by crystallization from cyclohexane yielded **BHA-3T** as orange solid (573 mg, 78%). ^{1}H NMR (200 MHz, CD_2Cl_2/CS_2): δ = 7.48 (4 H, d, J = 8.8 Hz), 7.34 - 7.22 (8 H, m), 7.19 - 7.00 (22 H. m) ppm. ^{13}C NMR (50 MHz, CD_2Cl_2/CS_2): δ = 148.0 (s), 147.9 (s), 143.8 (s), 136.7 (s), 136.0 (s), 129.8 (d), 128.4 (s), 127.0 (d), 125.2 (d), 125.2 (d), 124.7 (d), 124.0 (d), 123.8 (d), 123.5 (d) ppm. MS (MALDI-TOF): calcd for $C_{48}H_{34}N_2S_3$: 734.1884; found: 734.1750.

4,4'-(2,2':5',2''-Terthiophene-5,5''-diyl)bis[*N,N*-bis(4-methylphenyl)benzenamine] - **BpMA-3T**

According to the general procedure **BpMA-3T** was synthesized applying 5,5'-dibromo-2,2':5',2''-terthiophene (406 mg, 1.0 mmol, 1.0 eq), boronic ester of BpMA (1198 mg, 3.0 mmol, 3.0 eq), KOtBu (337 mg, 3.0 mmol, 3.0 eq) and (IPr)Pd(allyl)Cl (11 mg, 20 µmol; dissolved in 2 mL IPA) were suspended in a mixture of 24 mL degassed IPA : H_2O (3 : 1). The reaction mixture was refluxed until complete conversion (1.5 h). After standard workup the crude product was loaded upon silica gel (6 g) and column chromatography (90 g silica gel) using cyclohexane : DCM = 9 - 17% followed by crystallization from cyclohexane : benzene 9 : 1 yielded **BpMA-3T** as orange solid (687 mg, 87%). ^{1}H NMR (200 MHz, CD_2Cl_2): δ = 7.43 (4 H, d, J = 8.6 Hz), 7.18 - 7.05 (14 H, m), 7.04 - 6.90 (12 H, m), 2.32 (12 H, s) ppm. ^{13}C NMR (50 MHz, CD_2Cl_2): δ = 148.5 (s), 145.4 (s), 143.9 (s), 136.6

(s), 135.6 (s), 133.7 (s), 130.5 (d), 127.3 (s), 126.7 (d), 125.5 (d), 125.1 (d), 124.5 (d), 123.2 (d), 122.6 (d), 21.1 (q) ppm. MS (MALDI-TOF): calcd for $C_{52}H_{42}N_2S_3$: 790.2510; found: 790.260.

4,4'-(2,2':5',2''-Terthiophene-5,5''-diyl)bis[*N,N*-bis(4-methoxyphenyl)benzenamine] - **BMOA-3T**

According to the general procedure **BMOA-3T** was synthesized applying 5,5'-dibromo-2,2':5',2''-terthiophene (406 mg, 1.0 mmol, 1.0 eq), boronic ester of BMOA (1294 mg, 3.0 mmol, 3.0 eq), KOtBu (337 mg, 3.0 mmol, 3.0 eq) and (IPr)Pd(allyl)Cl (11 mg, 20 µmol; dissolved in 2 mL IPA) were suspended in a mixture of 16 mL degassed IPA : H_2O (3 : 1). The reaction mixture was refluxed until complete conversion (1.5 h). After standard workup the crude product was loaded upon silica gel (6 g) and column chromatography (90 g silica gel) using light petroleum : DCM = 16 - 100% followed by crystallization from cyclohexane : benzene 9 : 1 yielded **BMOA-3T** as orange solid (724 mg, 85%). ^{1}H NMR (200 MHz, CD_2Cl_2): δ = 7.40 (4 H, d, J = 8.8 Hz), 7.16 - 7.00 (14 H, m), 6.94 - 6.79 (12 H, m), 3.79 (12 H, s) ppm. ^{13}C NMR (50 MHz, CD_2Cl_2): δ = 156.9 (s), 149.1 (s), 144.1 (s), 141.0 (s), 136.6 (s), 135.4 (s), 127.4 (d), 126.7 (d), 126.2 (s), 125.1 (d), 124.5 (d), 122.9 (d), 120.6 (d), 115.3 (d), 56.0 (q) ppm. MS (MALDI-TOF): calcd for $C_{52}H_{42}N_2O_4S_3$: 854.2307; found: 854.2266.

4,4'-(2,2':5',2''-Terthiophene-5,5''-diyl)bis[*N,N*-bis(4-fluorophenyl)benzenamine] - **BFA-3T**

According to the general procedure **BFA-3T** was synthesized applying 5,5'-dibromo-2,2':5',2''-terthiophene (406 mg, 1.0 mmol, 1.0 eq), boronic ester of BFA (1222 mg, 3.0 mmol, 3.0 eq), KOtBu (337 mg, 3.0 mmol, 3.0 e) and (IPr)Pd(allyl)Cl (11 mg, 20 µmol; dissolved in 2 mL IPA) were suspended in a mixture of 20 mL degassed IPA : H_2O (3 : 1). The reaction mixture was refluxed until complete conversion (1.5 h). After standard workup the crude product was loaded upon silica gel (6 g) and column chromatography (90 g silica gel) using cyclohexane : DCM = 8 - 20% followed by crystallization from cyclohexane : benzene 9 : 1 yielded **BFA-3T** as orange solid (704 mg, 82%). ^{1}H NMR (200 MHz, CD_2Cl_2): δ = 7.46 (4 H, d, J = 8.8 Hz), 7.18 - 6.92 (26 H, m) ppm. ^{13}C NMR (100 MHz, CD_2Cl_2): δ = 159.7 (s, J_{CF} = 242.3 Hz), 148.2 (s), 144.0 (s, J_{CF} = 2.9 Hz), 143.6 (s), 136.6 (s), 135.9 (s), 128.0 (s), 127.0 (d, J_{CF} = 8.1 Hz), 126.9 (d), 124.9 (d), 123.4 (d), 122.8 (d), 116.7 (d, J_{CF} = 22.5 Hz) ppm. MS (MALDI-TOF): calcd for $C_{48}H_{30}F_4N_2S_3$: 806.1507; found: 806.1512.

4,4'-(Thieno[3,2-*b*]thiophene-2,5-diyl)bis[(*N,N*-diphenyl)benzenamine] - **BHA-TT**

According to the general procedure **BHA-TT** was synthesized applying 2,5-dibromothieno[3,2-*b*]thiophene (596 mg, 2.0 mmol, 1.0 eq), boronic ester of BHA (2228 mg, 6.0 mmol, 3.0 eq), KOtBu (673 mg, 6.0 mmol, 3.0 eq) and (IPr)Pd(allyl)Cl (23 mg, 40 µmol; dissolved in 2 mL IPA) were suspended in a mixture of 40 mL degassed IPA : H_2O (3:1). The reaction mixture was refluxed until complete conversion (2 h). After standard workup the reaction mixture was loaded upon silica gel (7 g) and column chromatography using light petroleum : DCM = 5 - 50% followed by crystallization from n-hexane yielded **BHA-TT** as yellow crystals (1.091 g, 87%). Rf = 0.38 (light petroleum : DCM = 4 : 1). ^{1}H NMR (400 MHz, pyridine-d5): δ = 7.71 – 7.68 (6 H, m), 7.37 – 7.33 (8 H, m), 7.10 - 7.21 (16 H, m) ppm. ^{13}C NMR (100 MHz, pyridine-d5): δ = 148.4 (s), 148.3 (s), 146.3 (s), 139.9 (s), 130.4 (d), 129.6 (s), 127.4 (d), 125.5 (d), 124.5 (d), 124.3 (d), 116.0 (d) ppm. MS (MALDI-TOF): calcd for $C_{42}H_{30}N_2S$: 626.1850; found: 626.1699.

4,4'-(Thieno[3,2-*b*]thiophene-2,5-diyl)bis[*N,N*-bis(2-methylphenyl)benzenamine] - **BoMA-TT**

According to the general procedure **BoMA-TT** was synthesized applying 2,5-dibromothieno[3,2-*b*]thiophene (298 mg, 1.0 mmol, 1.0 eq), boronic ester of BoMA (1198 mg, 3.0 mmol, 3.0 eq), KOtBu (337 mg, 3.0 mmol, 3.0 eq) and (IPr)Pd(allyl)Cl (11 mg, 20 µmol; dissolved in 2 mL IPA) were suspended in a mixture of 20 mL degassed IPA : H_2O (3 : 1). The reaction mixture was refluxed until complete conversion (2 h). After standard workup the crude product was loaded upon silica gel (6.3 g) and column chromatography using light petroleum : DCM = 5 - 18% followed by crystallization from cyclohexane yielded **BoMA-TT** as yellow solid (360 mg, 53%). Rf = 0.33 (light petroleum : DCM = 5 : 1). ^{1}H NMR (400 MHz, CD_2Cl_2): δ = 7.43 (4 H, d, J = 8.8 Hz), 7.33 (2 H, brs), 7.24 (4 H, d, J = 8.2 Hz), 7.06 - 7.20 (8 H, m), 7.00 (4 H, d, J = 8.2 Hz), 6.65 (4 H, d, J = 8.8 Hz), 2.06 (12 H, s) ppm. ^{13}C NMR (100 MHz, CD_2Cl_2): δ = 148.9, 146.1, 139.0, 135.5, 132.3, 128.1, 127.6, 127.1, 126.8, 125.7, 120.1, 114.5, 19.2 ppm. MS (MALDI-TOF): calcd for $C_{46}H_{38}N_2S_2$: 682.2476; found: 682.2272.

9,9'-(Thieno[3,2-*b*]thiophene-2,5-diyl-di-4,1-phenylene)bis(9*H*-carbazole) - **PCz-TT**

According to the general procedure **PCz-TT** was synthesized applying 2,5-dibromothieno[3,2-*b*]thiophene (596 mg, 2.0 mmol, 1.0 eq), boronic ester of PCz (2216 mg, 6.0 mmol, 3.0 eq), KOtBu (673 mg, 6.0 mmol, 3.0 eq) and (IPr)Pd(allyl)Cl (23 mg, 40 µmol; dissolved in 2 mL IPA) were suspended in a mixture of 40 mL degassed IPA : H_2O (3:1). The reaction mixture was refluxed until complete conversion (3 h). After standard workup the product was purified by crystallization from pyridine yielding **PCz-TT** as yellow goldish solid (745 mg, 60%). Rf= 0.33 (light petroleum : DCM). ^{1}H NMR (400 MHz, pyridine-d_5): δ = 8.33 (4 H, d, J = 7.9 Hz), 8.07 (4 H, d, J = 8.2 Hz), 7.98 (2 H, s), 7.64 (4 H, d, J = 8.5 Hz), 7.51 - 7.57 (8 H, m), 7.40 - 7.46 (4 H, m) ppm. ^{13}C NMR (100 MHz, pyridine-d5): δ = 146.3, 141.7, 141.2, 138.1, 134.8, 128.5, 128.3, 127.4, 124.8, 121.7, 121.5, 118.0, 111.1 ppm. MS (MALDI-TOF): calcd for $C_{42}H_{26}N_2S_2$: 622.1537; found: 622.1442.

2,2'-(Thieno[3,2-*b*]thiophene-2,5-diyl)bis(indolo[3,2,1-*jk*]carbazol) - **ICz-TT**

According to the general procedure **ICz-TT** was synthesized applying 2,5-dibromothieno[3,2-*b*]thiophene (298 mg, 1.0 mmol, 1.0 eq), boronic ester of ICz (1100 mg, 3.0 mmol, 3.0 eq), KOtBu (337 mg, 3.0 mmol, 3.0 eq) and (IPr)Pd(allyl)Cl (11 mg, 20 µmol; dissolved in 2 mL IPA) were suspended in a mixture of 40 mL degassed IPA : H_2O (3:1). The reaction mixture was refluxed until complete conversion (2 h). After standard workup the product was purified by crystallization from pyridine yielding **ICz-TT** as yellow solid (293 mg, 47%). Rf = 0.18 (light petroleum : DCM = 5 : 1). MS (MALDI-TOF): calcd for $C_{42}H_{22}N_2S_2$: 618.1224; found: 618.1073.

4,4'-(Dithieno[3,2-*b*:2',3'-*d*]thiophene-2,6-diyl)bis(*N,N*-diphenylbenzenamine) - **BHA-DTT**

According to the general procedure **BHA-DTT** was synthesized applying 2,6-dibromodithieno[3,2-*b*:2',3'-*d*]thiophene (354 mg, 1.0 mmol, 1.0 eq), boronic ester of BHA (1114 mg, 3.0 mmol, 3.0 eq), KOtBu (337 mg, 3.0 mmol, 3.0 eq) and (IPr)Pd(allyl)Cl (11 mg, 20 µmol; dissolved in 2 mL IPA) were suspended in a mixture of 15 mL degassed IPA : H_2O (3 : 1). The reaction mixture was refluxed until complete conversion (2 h). After standard workup the reaction mixture was loaded upon silica gel (7 g) and column chromatography (90 g silica gel) using light petroleum : DCM = 15 - 40% followed by crystallization from cyclohexane yielded **BHA-DTT** as yellow solid (560 mg, 82%). ^{1}H NMR (400 MHz, CD_2Cl_2): δ = 7.52 (4 H, d, J = 8.5 Hz), 7.45 (2 H, s), 7.31 – 7.27 (8 H, m), 7.12 (8 H, d, J = 7.9 Hz), 7.02 - 7.10 (8 H, m) ppm. ^{13}C NMR (100 MHz, CD_2Cl_2): δ = 148.3 (s), 147.9 (s), 145.4 (s), 142.2 (s), 130.1 (s), 129.9 (s), 128.8 (s), 126.9 (s), 125.3 (s), 123.9 (s), 116.1 (s) ppm. MS (MALDI-TOF): calcd for $C_{44}H_{30}N_2S_3$: 682.1571; found: 682.1445.

4,4'-(Dithieno[3,2-*b*:2',3'-*d*]thiophene-2,6-diyl)bis[*N,N*-bis(2-methylphenyl)benzenamine] - **BoMA-DTT**

According to the general procedure **BoMA-DTT** was synthesized applying 2,6-dibromodithieno[3,2-*b*:2',3'-*d*]thiophene (354 mg, 1.0 mmol, 1.0 eq), boronic ester of BoMA (1198 mg, 3.0 mmol, 3.0 eq), KOtBu (337 mg, 3.0 mmol, 3.0 eq) and (IPr)Pd(allyl)Cl (11 mg, 20 µmol; dissolved in 2 mL IPA) were suspended in a mixture of 40 mL degassed IPA : H_2O (3 : 1). The reaction mixture was refluxed until complete conversion (2 h). After standard workup the crude product was loaded upon silica gel (6.5 g) and column chromatography (90g silica gel) using light petroleum : DCM = 8 - 30% followed by crystallization from cyclohexane yielded **BoMA-DTT** as yellow solid (679 mg, 92%). Rf = 0.10 (light petroleum : DCM = 9 : 1). ^{1}H NMR (200 MHz, CD_2Cl_2): δ = 7.45 (4 H, d, J = 8.8 Hz), 7.37 (2 H, d, J = 6.7 Hz), 7.19 - 7.29 (4 H, m), 7.05 - 7.19 (8 H, m), 7.02 (2 H, d, J = 2.4 Hz), 6.96 - 7.00 (2 H, m), 6.65 (4 H, d, J = 8.8 Hz), 2.07 (12 H, s) ppm. ^{13}C NMR (50 MHz, CD_2Cl_2): δ = 149.0 (s), 146.0 (s), 145.7 (s), 142.0 (s), 135.5 (s), 132.3 (d), 129.7 (s), 128.1 (d), 127.6 (d), 126.8 (d), 125.7 (d), 120.1 (d), 115.5 (d), 19.2 (q) ppm. MS (MALDI-TOF): calcd for $C_{48}H_{38}N_2S_3$: 738.2197; found: 738.2114.

9,9'-(Dithieno[3,2-*b*:2',3'-*d*]thiophene-2,6-diyl-di-4,1-phenylene)bis(9*H*-carbazole) - **PCz-DTT**

According to the general procedure **PCz-DTT** was synthesized applying 2,6-dibromodithieno[3,2-*b*:2',3'-*d*]thiophene (708 mg, 2.0 mmol, 1.0 eq), boronic ester of PCz (2216 mg, 6.0 mmol, 3.0 eq), KOtBu (673 mg, 6.0 mmol, 3.0 eq) and (IPr)Pd(allyl)Cl (23 mg, 40 µmol; dissolved in 2 mL IPA) were suspended in a mixture of 40 mL degassed IPA : H_2O (3 : 1). The reaction mixture was refluxed until complete conversion (3 h). After standard workup the crude product was purified by crystallization from pyridine yielding **PCz-DTT** as bright yellow solid (790 mg, 58%). ^{1}H NMR (400 MHz, CD_2Cl_2): δ = 8.13 - 8.21 (4 H, m), 7.93 (4 H, s), 7.71 (2 H, s), 7.68 (4 H, d, J = 8.4 Hz), 7.51 (4 H, d, J = 7.7 Hz), 7.45 (4 H, t, J = 7.3 Hz), 7.32 (4 H, t, J = 8.8 Hz) ppm. MS (MALDI-TOF): calcd for $C_{44}H_{26}N_2S_3$: 678.1258; found: 678.1226.

2,2'-(Dithieno[3,2-*b*:2',3'-*d*]thiophene-2,6-diyl)bis(indolo[3,2,1-*jk*]carbazole) - **ICz-DTT**

According to the general procedure **ICz-DTT** was synthesized applying 2,6-dibromodithieno[3,2-*b*:2',3'-*d*]thiophene (354 mg, 1.0 mmol, 1.0 eq), boronic ester of ICz (1100 mg, 3.0 mmol, 3.0 eq), KOtBu (337 mg, 3.0 mmol, 3.0 eq) and (IPr)Pd(allyl)Cl (11 mg, 20 µmol; dissolved in 2 mL IPA) were suspended in a mixture of 40 mL degassed IPA : H_2O (3 : 1). The reaction mixture was refluxed until complete conversion (2 h). After standard workup the product was purified by crystallization from pyridine (500 mL) yielding **ICz-DTT** as dark yellow solid (360 mg, 53%).

MS (MALDI-TOF): calcd for $C_{44}H_{22}N_2S_3$: 674.0945; found: 674.1282.

4,4'-(2,2':5',2'':5'',2'''-Quaterthiophene-5,5'''-diyl)bis(*N,N*-diphenylbenzenamine) - **BHA-4T**

The synthesis of **BHA-4T** was realized microwave assisted at 120 °C applying 5,5'''-dibromo-2,2':5',2'':5'',2'''-quaterthiophene (122 mg, 0.25 mmol, 1.0 eq), boronic ester of BHA (278 mg, 0.75 mmol, 3.0 eq), KOtBu (84 mg, 0.25 mmol, 3.0 eq) and (IPr)Pd(allyl)Cl (2.9 mg, 2 µmol; dissolved in 1 mL IPA) in a mixture of 3 mL degassed IPA : H_2O (3 : 1) for 4 h. After standard workup the crude product was loaded upon silica gel (2.5 g) and column chromatography (45 g silica gel) using cyclohexane : DCM = 14 - 100% yielded **BHA-4T** as orange solid (65 mg, 29%). MS (MALDI-TOF): calcd for $C_{52}H_{36}N_2S_4$: 816.1761; found: 816.1741.

4,4'-(2,2':5',2'':5'',2'''-Quaterthiophene-5,5'''-diyl)bis[*N,N*-bis(4-methylphenyl)benzenamine] - **BpMA-4T**

The synthesis of **BpMA-4T** was realized microwave assisted at 120 °C applying 5,5'''-dibromo-2,2':5',2'':5'',2'''-quaterthiophene (122 mg, 0.25 mmol, 1.0 eq), boronic ester of BpMA (300 mg, 0.75 mmol, 3.0 eq), KOtBu (84 mg, 0.25 mmol, 3.0 eq) and (IPr)Pd(allyl)Cl (2.9 mg, 2 µmol; dissolved in 1 mL IPA) in a mixture of 3 mL degassed IPA : H_2O (3 : 1) for 4 h. After standard workup the crude product was loaded upon silica gel (2.5 g) and column chromatography (45 g silica gel) using cyclohexane : DCM = 14 - 100% yielded **BpMA-4T** as orange solid (120 mg, 54%). ^{1}H NMR (400 MHz, CD_2Cl_2): δ = 7.43 (4 H, d, J = 8.4 Hz), 7.14 (4 H, s), 7.11 - 7.09 (12 H, m), 7.01 - 6.96 (12 H, m), 2.32 (12 H, s) ppm. ^{13}C NMR (100 MHz, CD_2Cl_2): δ = 148.6 (s), 145.4 (s), 144.1 (s), 137.0 (s), 136.1 (s), 135.5 (s), 133.8 (s), 130.5 (d), 127.2 (s), 126.7 (d), 125.5 (d), 125.3 (d), 124.9 (d), 124.6 (d), 123.2 (d), 122.5 (d), 21.1 (q) ppm. MS (MALDI-TOF): calcd for $C_{56}H_{44}N_2S_4$: 872.2387; found: 872.2389.

4,4'-(2,2':5',2'':5'',2'''-Quaterthiophene-5,5'''-diyl)bis[*N,N*-bis(4-methoxyphenyl)benzenamine] - **BMOA-4T**

The synthesis of **BMOA-4T** was realized microwave assisted at 120 °C applying 5,5'''-dibromo-2,2':5',2'':5'',2'''-quaterthiophene (122 mg, 0.25 mmol, 1.0 eq), boronic ester of BMOA (324 mg, 0.75 mmol, 3.0 eq), KOtBu (84 mg, 0.25 mmol, 3.0 eq) and (IPr)Pd(allyl)Cl (2.9 mg, 2 µmol; dissolved in 1 mL IPA) in a mixture of 3 mL degassed IPA : H_2O (3 : 1) for 4 h. After standard workup the crude product was loaded upon silica gel (2.5 g) and column chromatography (45 g silica gel) using cyclohexane : DCM = 10 - 100% yielded **BMOA-4T** as red solid (112 mg, 48%).^{1}H NMR (200 MHz, CD_2Cl_2): δ = 7.41 (4 H, d, J = 8.6 Hz), 7.19 - 7.00 (16 H, m), 6.95 - 6.80 (12 H, m), 3.79 (12 H, s) ppm. ^{13}C NMR (100 MHz, CD_2Cl_2): δ = 156.8, 149.1, 144.3, 140.9, 137.0, 135.9, 135.2, 127.4, 126.6, 126.1, 125.2, 124.8, 124.4, 122.9, 120.5, 115.2, 56.0 ppm. MS (MALDI-TOF): calcd for $C_{56}H_{44}N_2O_4S_4$: 936.2184; found: 936.2422.

4,4'-(2,2':5',2'':5'',2'''-Quaterthiophene-5,5'''-diyl)bis[*N,N*-bis(4-fluorophenyl)benzenamine] - **BFA-4T**

The synthesis of **BFA-4T** was realized microwave assisted at 120 °C applying 5,5'''-dibromo-2,2':5',2'':5'',2'''-quaterthiophene (122 mg, 0.25 mmol, 1.0 eq), boronic ester of BFA (305 mg, 0.75 mmol, 3.0 eq), KOtBu (84 mg, 0.25 mmol, 3.0 eq) and (IPr)Pd(allyl)Cl (2.9 mg, 2 µmol; dissolved in 1 mL IPA) in a mixture of 3 mL degassed IPA : H_2O (3 : 1) for 4 h. After standard workup the crude product was loaded upon silica gel (2.5 g) and column chromatography (45 g silica gel) using cyclohexane : DCM = 10 - 100% yielded **BFA-4T** as red solid (75 mg, 34%). MS (MALDI-TOF): calcd for $C_{52}H_{32}F_4N_2S_4$: 888.1384; found: 888.1388.

2-Methyl-*N*-(2-methylphenyl)benzenamine - **1**

A modified protocol of Ackermann was applied.[63] In a three-necked flask 2-bromotoluene (42.75 g, 250 mmol, 1 eq) and 2-methylaniline (32.15 g, 300 mmol, 1.2 eq) were well stirred in 500 mL of anhydrous toluene and under argon atmosphere, before KOtBu (36.47 g, 325 mmol, 1.3 eq) was quickly added in small portions. The reddish orange suspension was refluxed for 30 min before (IPr)Pd(allyl)Cl (1.43 g, 2.5 mmol, 0.01 eq) was added quickly. The mixture was kept under reflux conditions until complete conversion (2 h). Et_2O (100 mL) and brine (100 mL) were added to the cooled reaction mixture. The separated aqueous phase was extracted repeatedly with Et_2O (3 x 50 mL). The combined organic layer were dried over Na_2SO_4 and concentrated in vacuo. The remaining residue was purified by flash column chromatography on silica gel (light petroleum : ethyl acetate = 20:1; 350 g) to yield **1** as an orange liquid which solidified upon standing (37.11 g, 75%). Rf = 0.37 (light petroleum : ethyl acetate = 20 : 1). ^{1}H NMR (200 MHz, $CDCl_3$): δ = 7.30 - 7.17 (4 H, m), 7.09 – 6.95 (4 H, m), 5.23 (1 H, s.) 2.35 (6 H, s) ppm.

N,N-bis(2-methylphenyl)-4-nitrobenzenamine - **2b**

In a three-necked flask equipped with a mechanical stirrer **1** (19.73 g, 100 mmol, 1 eq) and NaH (7.20 g, 300 mmol, 3 eq) were stirred at 50 °C in 300 mL of anhydrous DMF for 30 min under argon atmosphere. Then 4-fluoronitrobenzene (21.17 g, 150 mmol, 1.5 eq) dissolved in 200 mL of DMF was added dropwise. The reaction was

stirred at 50 °C until complete conversion (3 h) before DMF was removed in vacuo. DCM (300 mL) and H_2O (300 mL) were added to the reaction mixture. The separated aqueous phase was extracted repeatedly with DCM (3 x 50 mL). The combined organic layer was dried over Na_2SO_4 and concentrated in vacuo yielding a brown liquid. The product was purified by flash chromatography (200 g, light petroleum : Et_2O = 20 : 1) followed by recrystallization from light petroleum, yielding **2b** as yellow solid (23.42 g, 74%). Rf = 0. 71 (light petroleum : ethyl acetate = 5 : 1). ^{1}H NMR (200 MHz, $CDCl_3$): δ = 7.99 (2 H, d, J = 9.2 Hz), 7.26 - 7.10 (6 H, m), 7.04 – 6.95 (2 H, m), 6.48 (2 H, d, J = 9.2 Hz) 2.06 (6 H, s) ppm. ^{13}C NMR (50 MHz, $CDCl_3$): δ = 153.3 (s), 143.5 (s), 139.5 (s), 135.0 (s), 132.0 (d), 128.0 (d), 127.6 (d), 126.7 (d), 125.7 (d), 116.0 (d), 18.8 (q) ppm.

N,N-Bis(2-methylphenyl)-1,4-benzenediamine - **2c**

Synthesis of **2c** followed a protocol by Chen.[40] To a solution of **2b** (22.92 g, 72 mmol, 1 eq) in 250 mL of EtOH, $SnCl_2 \cdot 2H_2O$ (56.86 g, 252 mmol, 3.5 eq) was added quickly and then heated under reflux until complete conversion (6 h). Most of the ethanol was distilled off under reduced pressure, and the solution was alkalized by adding 40 wt% NaOH (50 mL) dropwise under stirring and yellow solid precipitated. The resulting mixture was extracted with toluene and washed with water. The combined toluene extracts were dried over Na_2SO_4 and the solvent was removed under reduced pressure. Orange yellowish solid product **2c** was obtained (20.9 g, 99%). Rf = 0.30 (light petroleum : ethyl acetate = 5 : 1). ^{1}H NMR (200 MHz, CD_2Cl_2): δ = 7.19 – 6.96 (6 H, m), 6.85 (2 H, dd, J = 7.6, 1.6 Hz), 6.61 – 6.52 (4 H, m), 3.52 (2 H, bs), 1.97 (6 H, s) ppm. ^{13}C NMR (50 MHz, CD_2Cl_2): δ = 148.0 (s), 141.9 (s), 141.5 (s), 134.5 (s), 132.0 (d), 127.1 (d), 126.8 (d), 124.2 (d), 124.0 (d), 116.2 (d), 19.2 (q) ppm.

4-Iodo-*N,N'*-bis(2-methylphenyl)benzenamine - **2d**

A solution of **2c** (14.42 g, 50 mmol, 1 eq) in ACN (80 mL), and H_2O (80 mL) was stirred in an ice bath while concentrated HCl (25 mL, 6 eq) was added dropwise over 5 min. To this mixture, still in an ice bath, was added a solution of $NaNO_2$ (6.90 g, 100 mmol, 2 eq) in 80 mL of H_2O keeping the temperature between -5 to 0 °C. The reaction mixture turned from orange to green and was stirred at that temperature for 1 h. After that a solution of KI (41.50 g, 250 mmol, 5 eq) in 80 mL of H_2O was added quickly. The red reaction mixture was then heated to reflux until no more purple or brown vapor was evolved. After complete conversion (2 h), ACN was removed in vacuo and the reaction was neutralized with 2N NaOH (200 mL). The black aqueous phase turned yellow and was extracted with $CHCl_3$ (3 x 100 mL). The combined organic layer was washed with a saturated solution of $Na_2S_2O_5$ and dried over Na_2SO_4. The solvent was removed in vacuo yielding black tar. The product was purified via flash chromatography (light petroleum) followed by crystallization from MeOH : ACN = 100 : 1 yielding **2d** as slightly yellow solid (15.17 g, 76%). ^{1}H NMR (400 MHz, $CDCl_3$): δ = 7.43 (2 H, d, J = 9.2 Hz), 7.22 (2 H, d, J = 7.0 Hz), 7.16 - 7.07 (4 H, m), 6.97 (2 H, d, J = 8.8 Hz), 6.44 (2 H, d, J = 8.8 Hz), 2.03 (6 H, s) ppm. ^{13}C NMR (100 MHz, $CDCl_3$): δ = 148.3 (s), 145.3 (s), 137.6 (d), 134.6 (s), 131.7 (d), 127.4 (d), 127.0 (d), 125.1 (d), 121.5 (d), 82.0 (s), 18.9 (q) ppm.

2-Methyl-*N*-(2-methylphenyl)-*N*-[4-(4,4,5,5-tetramethyl-1,3,2-dioxaborolan-2-yl)phenyl] benzenamine (boronic ester of BoMA)

Synthesis was done according to Murata.[41] **2d** (6.15 g, 15.4 mmol, 1.0 eq) and $PdCl_2$(dppf) (0.338 g, 0.46 mmol, 0.03 eq) were dissolved in anhydrous dioxane (60 mL). The mixture was heated to 80 °C under argon atmosphere. Pinacolborane (2.56 g, 20 mmol, 1.3 eq) and Et_3N (4.68 g, 46 mmol, 3 eq) were added dropwise and the reaction was stirred until complete conversion (1 h). The solvent was removed under reduced pressure and the dark residue was purified by column chromatography (light petroleum : ethyl acetate = 100 : 3). Finally, the product was crystallized from ACN yielding target compound as a white solid (3.97 g, 65%). ^{1}H NMR (400 MHz, CD_2Cl_2): δ = 7.55 (2 H, d, J = 8.5 Hz), 7.24 (2 H, dd, J = 7.3, 1.17 Hz), 7.17 - 7.10 (4 H, m), 6.99 (2 H, d, J = 7.3 Hz), 6.58 (2 H, d, J = 8.8 Hz), 2.05 (6 H, s), 1.31 (12 H, s) ppm. ^{13}C NMR (100 MHz, CD_2Cl_2): δ = 151.5 (s), 145.9 (s), 136.2 (d), 135.7 (s), 132.2 (d), 128.4 (d), 127.6 (d), 125.8 (d), 118.4 (d), 83.9 (s), 25.2 (q), 19.2 (q) ppm.

Computational details

All density functional theory (DFT) and time-dependent (TD) DFT calculations were performed with Gaussian G09.Rev.A02.[64] Ground and first excited state geometries were optimized using a combination of M06-2X functional[27] and the polarized double zeta SVP basis set.[65] In a previous study[31] it was found that M06-2X was superior to functionals with a smaller amount of Hartree-Fock exchange (i.e. B3LYP[66,67] and PBE0[68,69]). This need of including Hartree-Fock exchange can be traced back to dynamic charge separation occurring in large conjugated systems.[70,71] As opposed to the functional, the basis set was found to play only a minor role, and the addition of diffuse basis functions only caused a modest redshift of about 0.1 eV.[31] All minima were verified by normal mode analysis. Solvent effects were considered through the polarizable continuum model (PCM)[45] in its linear response (LR-PCM)[46] and state specific (SS-PCM)[47] formulations, always considering the equilibrium time regime (eq) for the excited state. Spectra simulations were performed within the Newton-X framework (version 1.2.4.).[72] As Newton-X is for simplicity limited to the LR-PCM model, spectra were simulated including the vibrational broadening with this model first using a Wigner distribution formalism, as described in Ref.[73] applying a phenomenological broadening of δ = 0.1 eV. Taking the output of the frequency analysis of S1 as the source of the normal modes, this information is used to provide a selectable number of non-equilibrium geometries, in these particular cases 250. The S1 → S0 excitation energy for each geometry was calculated using the M06-2X/SVP parametrization at TDDFT level of theory applying LR-PCM solvent correction. Notably these are all independent single point calculations which can easily be spread to a large number of compute nodes thus significantly reducing wall clock time. Afterwards data is combined to construct a vibrationally broadened spectrum, already having solvent effects at LR-PCM level included. However, as further improvement of the methodology, the SS-PCM solvent influence was included as a post processing correction consecutive to the spectrum simulation. In order to achieve this, we made the assumption that the energy difference between the LR-PCM and SS-PCM approach is constant for all the 250 geometries used for spectra simulation throughout the whole spectral range (which of course is a simplification of the model). Hence, the results of the single point calculations performed within the framework of NEWTON-X were in turn corrected by the difference between LR- and SS- results calculated for the vertical emission at the S1 equilibrium geometry to finally obtain spectra which both include the more accurate SS-PCM correction as well as the vibrational broadening.

Acknowledgements

JB is grateful for the Marietta Blau Grant of the OeAD (ICM201400009). FP is supported by the VSC Research Center funded by the Austrian Federal Ministry of Science, Research, and Economy (bmwfw). This material is based upon work supported by the NSF MRSEC program through Columbia in the Center for Precision Assembly of Superstratic and Superatomic Solids (DMR-1420634). Andreas Gaubitzer, Barbara Pokorny, Christian Aumayer and Rene Klaffenböck are gratefully acknowledged for their synthetic help.

Keywords: structure property relationship • computational guided synthesis • fluorescent compounds • OLED • modified triarylamines

[1] S. Reineke, F. Lindner, G. Schwartz, N. Seidler, K. Walzer, B. Lüssem, K. Leo, *Nature* **2009**, *459*, 234.
[2] Y. Sun, N. C. Giebink, H. Kanno, B. Ma, M. E. Thompson, S. R. Forrest, *Nature* **2006**, *440*, 908.
[3] J.-S. Park, H. Chae, H. K. Chung, S. I. Lee, *Semicond. Sci. Technol.* **2011**, *26*, 034001.
[4] K. T. Kamtekar, A. P. Monkman, M. R. Bryce, *Adv. Mater.* **2010**, *22*, 572.
[5] H. Klauk, Ed. , *Organic Electronics. [1]: Materials, Manufacturing and Applications*, Wiley-VCH, Weinheim, **2008**.
[6] H. Klauk, Ed. , *Organic Electronics. 2: More Materials and Applications*, Wiley-VCH-Verl, Weinheim, **2012**.
[7] C. Murawski, K. Leo, M. C. Gather, *Adv. Mater.* **2013**, *25*, 6801.
[8] I. F. Perepichka, D. F. Perepichka, Eds. , *Handbook of Thiophene-Based Materials*, John Wiley & Sons, Ltd, Chichester, UK, **2009**.
[9] M. Halik, H. Klauk, U. Zschieschang, G. Schmid, S. Ponomarenko, S. Kirchmeyer, W. Weber, *Adv. Mater.* **2003**, *15*, 917.
[10] Q. Xia, M. Burkhardt, M. Halik, *Org. Electron.* **2008**, *9*, 1061.
[11] K. Oniwa, H. Kikuchi, H. Shimotani, S. Ikeda, N. Asao, Y. Yamamoto, K. Tanigaki, T. Jin, *Chem Commun* **2016**, *52*, 4800.
[12] J. Filo, R. Mišicák, M. Cigáň, M. Weis, J. Jakabovič, K. Gmucová, M. Pavúk, E. Dobročka, M. Putala, *Synth. Met.* **2015**, *202*, 73.
[13] Y. Shirota, *J. Mater. Chem.* **2000**, *10*, 1.
[14] N. Metri, X. Sallenave, C. Plesse, L. Beouch, P.-H. Aubert, F. Goubard, C. Chevrot, G. Sini, *J. Phys. Chem. C* **2012**, *116*, 3765.
[15] J. Zhang, D. Deng, C. He, Y. He, M. Zhang, Z.-G. Zhang, Z. Zhang, Y. Li, *Chem. Mater.* **2011**, *23*, 817.
[16] Z. Ning, H. Tian, *Chem. Commun.* **2009**, 5483.
[17] A. Iwan, D. Sek, D. Pociecha, A. Sikora, M. Palewicz, H. Janeczek, *J. Mol. Struct.* **2010**, *981*, 120.
[18] A. Iwan, D. Sek, *Prog. Polym. Sci.* **2011**, *36*, 1277.
[19] T. Noda, H. Ogawa, N. Noma, Y. Shirota, *Adv. Mater.* **1997**, *9*, 720.
[20] D. Lumpi, B. Holzer, J. Bintinger, E. Horkel, S. Waid, H. D. Wanzenböck, M. Marchetti-Deschmann, C. Hametner, E. Bertagnolli, I. Kymissis, J. Fröhlich, *New J Chem* **2015**, *39*, 1840.
[21] E. Runge, E. K. U. Gross, *Phys. Rev. Lett.* **1984**, *52*, 997.
[22] D. P. Chong, Ed. , *Recent Advances in Density Functional Methods*, World Scientific, Singapore ; River Edge, N.J, **1995**.
[23] A. Dreuw, M. Head-Gordon, *Chem. Rev.* **2005**, *105*, 4009.
[24] M. J. G. Peach, C. R. L. Sueur, K. Ruud, M. Guillaume, D. J. Tozer, *Phys. Chem. Chem. Phys.* **2009**, *11*, 4465.
[25] F. Plasser, M. Barbatti, A. J. A. Aquino, H. Lischka, *Theor. Chim. Acta* **2012**, *131*, 1073.
[26] A. D. Laurent, D. Jacquemin, *Int. J. Quantum Chem.* **2013**, *113*, 2019.
[27] Y. Zhao, D. G. Truhlar, *Theor. Chem. Acc.* **2008**, *119*, 525.
[28] D. Jacquemin, E. A. Perpète, I. Ciofini, C. Adamo, R. Valero, Y. Zhao, D. G. Truhlar, *J. Chem. Theory Comput.* **2010**, *6*, 2071.
[29] S. S. Leang, F. Zahariev, M. S. Gordon, *J. Chem. Phys.* **2012**, *136*, 104101.
[30] D. Jacquemin, A. Planchat, C. Adamo, B. Mennucci, *J. Chem. Theory Comput.* **2012**, *8*, 2359.
[31] D. Lumpi, E. Horkel, F. Plasser, H. Lischka, J. Fröhlich, *ChemPhysChem* **2013**, *14*, 1016.
[32] T. Noda, H. Ogawa, N. Noma, Y. Shirota, *J. Mater. Chem.* **1999**, *9*, 2177.
[33] D. A. Doval, M. D. Molin, S. Ward, A. Fin, N. Sakai, S. Matile, *Chem. Sci.* **2014**, *5*, 2819.
[34] P. Kautny, D. Lumpi, Y. Wang, A. Tissot, J. Bintinger, E. Horkel, B. Stöger, C. Hametner, H. Hagemann, D. Ma, J. Fröhlich, *J. Mater. Chem. C* **2014**, *2*, 2069.
[35] B. Holzer, M. Tromayer, M. Lunzer, D. Lumpi, E. Horkel, C. Hametner, A. Rosspeintner, E. Vauthey, R. Liska, J. Fröhlich, *Manuscr. Prep.* **n.d.**
[36] N.-X. Wang, *Synth. Commun.* **2003**, *33*, 2119.
[37] J. Roncali, M. Giffard, P. Frère, M. Jubault, A. Gorgues, *J. Chem. Soc. Chem. Commun.* **1993**, 689.
[38] J. Nakayama, T. Konishi, S. Murabayashi, M. Hoshino, *HETEROCYCLES* **1987**, *26*, 1793.
[39] J. Frey, A. D. Bond, A. B. Holmes, *Chem. Commun.* **2002**, 2424.
[40] Y.-C. Chen, G.-S. Huang, C.-C. Hsiao, S.-A. Chen, *J. Am. Chem. Soc.* **2006**, *128*, 8549.
[41] M. Murata, T. Oyama, S. Watanabe, Y. Masuda, *J. Org. Chem.* **2000**, *65*, 164.
[42] T. Noda, H. Ogawa, N. Noma, Y. Shirota, *Adv. Mater.* **1997**, *9*, 720.
[43] P. Kautny, Z. Wu, J. Eichelter, E. Horkel, B. Stöger, J. Chen, D. Ma, J. Fröhlich, D. Lumpi, *Org. Electron.* **2016**, *34*, 237.
[44] H. Puntscher, P. Kautny, B. Stöger, A. Tissot, C. Hametner, H. R. Hagemann, J. Fröhlich, T. Baumgartner, D. Lumpi, *RSC Adv.* **2015**, *5*, 93797.
[45] M. Cossi, V. Barone, R. Cammi, J. Tomasi, *Chem. Phys. Lett.* **1996**, *255*, 327.
[46] M. Cossi, V. Barone, *J. Chem. Phys.* **2001**, *115*, 4708.
[47] R. Improta, G. Scalmani, M. J. Frisch, V. Barone, *J. Chem. Phys.* **2007**, *127*, 074504.
[48] S. Corni, R. Cammi, B. Mennucci, J. Tomasi, *J. Chem. Phys.* **2005**, *123*, 134512.
[49] M. Caricato, B. Mennucci, J. Tomasi, F. Ingrosso, R. Cammi, S. Corni, G. Scalmani, *J. Chem. Phys.* **2006**, *124*, 124520.
[50] C. Daday, C. Curutchet, A. Sinicropi, B. Mennucci, C. Filippi, *J. Chem. Theory Comput.* **2015**, *11*, 4825.
[51] Š. Budzák, A. D. Laurent, C. Laurence, M. Medved', D. Jacquemin, *J. Chem. Theory Comput.* **2016**, *12*, 1919.
[52] O. Navarro, S. P. Nolan, *Synthesis* **2006**, 366.
[53] T. Hayashi, M. Konishi, Y. Kobori, M. Kumada, T. Higuchi, K. Hirotsu, *J. Am. Chem. Soc.* **1984**, *106*, 158.
[54] P. Liu, Y. Wu, H. Pan, Y. Li, S. Gardner, B. S. Ong, S. Zhu, *Chem. Mater.* **2009**, *21*, 2727.
[55] S. A. Odom, K. Lancaster, L. Beverina, K. M. Lefler, N. J. Thompson, V. Coropceanu, J.-L. Brédas, S. R. Marder, S. Barlow, *Chem. - Eur. J.* **2007**, *13*, 9637.
[56] H. Xu, K. Yin, W. Huang, *Chem. - Eur. J.* **2007**, *13*, 10281.
[57] R. Anémian, D. C. Cupertino, P. R. Mackie, S. G. Yeates, *Tetrahedron Lett.* **2005**, *46*, 6717.
[58] *Bruker computer programs: APEX2, SAINT and SADABS (Bruker AXS Inc., Madison, WI, 2015)* **n.d.**
[59] L. Palatinus, G. Chapuis, *J. Appl. Crystallogr.* **2007**, *40*, 786.
[60] V. Petříček, M. Dušek, L. Palatinus, *Z. Für Krist. - Cryst. Mater.* **2014**, *229*, 345.
[61] C. F. Macrae, P. R. Edgington, P. McCabe, E. Pidcock, G. P. Shields, R. Taylor, M. Towler, J. van de Streek, *J. Appl. Crystallogr.* **2006**, *39*, 453.
[62] N. Marion, O. Navarro, J. Mei, E. D. Stevens, N. M. Scott, S. P. Nolan, *J. Am. Chem. Soc.* **2006**, *128*, 4101.
[63] L. Ackermann, A. Althammer, P. Mayer, *Synthesis* **2009**, *2009*, 3493.
[64] M. J. Frisch, G. W. Trucks, H. B. Schlegel, G. E. Scuseria, M. A. Robb, J. R. Cheeseman, G. Scalmani, V. Barone, B. Mennucci, G. A. Petersson, H. Nakatsuji, M. Caricato, X. Li, H. P. Hratchian, A. F. Izmaylov, J. Bloino, G. Zheng, J. L. Sonnenberg, M. Hada, M. Ehara, K. Toyota, R. Fukuda, J. Hasegawa, M. Ishida, T. Nakajima, Y. Honda, O. Kitao, H. Nakai, T. Vreven, J. A. Montgomery Jr., J. E. Peralta, F. Ogliaro, M. J. Bearpark, J. Heyd, E. N. Brothers, K. N. Kudin, V. N. Staroverov, R. Kobayashi, J. Normand, K. Raghavachari, A. P. Rendell, J. C. Burant, S. S. Iyengar, J. Tomasi, M. Cossi, N. Rega, N. J. Millam, M. Klene, J. E. Knox, J. B. Cross, V. Bakken, C. Adamo, J. Jaramillo, R. Gomperts, R. E. Stratmann, O. Yazyev, A. J. Austin, R. Cammi, C. Pomelli, J. W. Ochterski, R. L. Martin, K. Morokuma, V. G. Zakrzewski, G. A. Voth, P. Salvador, J. J. Dannenberg, S. Dapprich, A. D. Daniels, Ö. Farkas, J. B. Foresman, J. V. Ortiz, J. Cioslowski, D. J. Fox, *Gaussian 09, Revision A.02*, Gaussian, Inc., Wallingford, CT, USA, **2009**.
[65] A. Schafer, H. Horn, R. Ahlrichs, *J. Chem. Phys.* **1992**, *97*, 2571.
[66] C. Lee, W. Yang, R. G. Parr, *Phys. Rev. B* **1988**, *37*, 785.
[67] A. D. Becke, *J. Chem. Phys.* **1993**, *98*, 5648.
[68] C. Adamo, V. Barone, *J. Chem. Phys.* **1999**, *110*, 6158.
[69] J. P. Perdew, K. Burke, M. Ernzerhof, *Phys. Rev. Lett.* **1996**, *77*, 3865.
[70] R. M. Richard, J. M. Herbert, *J. Chem. Theory Comput.* **2011**, *7*, 1296.
[71] S. A. Mewes, F. Plasser, A. Dreuw, *J. Chem. Phys.* **2015**, *143*, 171101.
[72] M. Barbatti, M. Ruckenbauer, F. Plasser, J. Pittner, G. Granucci, M. Persico, H. Lischka, *Wiley Interdiscip. Rev. Comput. Mol. Sci.* **2014**, *4*, 26.
[73] M. Barbatti, G. Granucci, M. Persico, M. Ruckenbauer, M. Vazdar, M. Eckert-Maksić, H. Lischka, *J. Photochem. Photobiol. Chem.* **2007**, *190*, 228.

Entry for the Table of Contents (Please choose one layout)

Layout 1:

ARTICLE

Computational chemistry guided synthesis for color tuning of OLED materials.

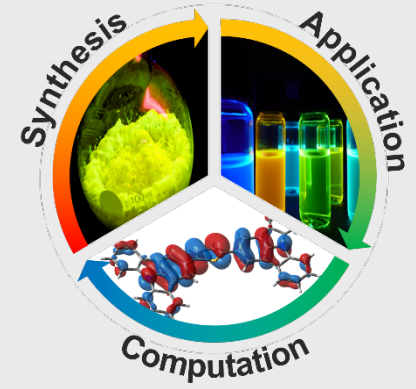

Brigitte Holzer[a], Johannes Bintinger[a,b]*‡, Daniel Lumpi[a], Chris Choi[b], Youngwan. Kim[b], Berthold Stöger[c], Christian Hametner[a], Martina Marchetti-Deschmann[c], Felix Plasser[d], Ernst Horkel[a]‡, Ioannis Kymissis[b] and Johannes Fröhlich[a]*

Page No. – Page No.

Color Fine Tuning of Optical Materials Through Rational Design

Layout 2:

ARTICLE

((Insert TOC Graphic here))

*Author(s), Corresponding Author(s)**

Page No. – Page No.

Title

Text for Table of Contents